IMMOBILE TRACE ELEMENT SYSTEMATICS OF OCEANIC ISLAND BASALTS: THE ROLE OF OCEANIC LITHOSPHERE IN CREATING THE GEOCHEMICAL DIVERSITY

Kaan Sayit

Department of Geological Sciences, San Diego State University, San Diego, CA 92182-1020, USA.
E-mail: kaansayit@gmail.com

Keywords: *End-members, trace element, mantle plume, OIB, oceanic basalts, mixing.*

ABSTRACT

The Earth's mantle is known to be heterogeneous at different scales, which has been generally linked to the presence of diverse mantle reservoirs, some of which are believed to have remained isolated for long periods of time. When oceanic island basalts (OIBs) are subdivided into five distinct end-member groups on the basis of Sr-Nd-Pb isotope systematics, which include DM, EM1, EM2, HIMU and C, trace element systematics do not appear to be effective discriminators as isotopes, though an end-member signature may become dominant relative to others within a specific ratio range. Melting of a lithologically heterogeneous source or melting of distinct sources, which is followed by melt mixing, appears to be an important mechanism in creating variable geochemical signatures in OIB genesis. Ratio-based trace element modeling suggests that sole involvement of eclogitic components cannot explain the entire elemental variation observed in OIBs; a peridotitic component must have been involved in the genesis of all types of end-member signatures. Combined trace element and isotope systematics are consistent with the involvement of metasomatized oceanic lithosphere (crust + lithospheric mantle) with/without sediments. This mechanism, which involves slab components uprising within the plumes, may also have been the main reason causing the geochemical diversity in the Tethyan mantle.

INTRODUCTION

It is well established that the earth's mantle is heterogeneous at variable scales (e.g., Dupre and Allègre, 1983; Hart, 1984; Zindler and Hart, 1986). This heterogeneity, which mainly reflects the effects of crustal and mantle recycling, has been commonly attributed to the presence of distinct "mantle reservoirs" or "end-members" generally believed to have been stored in the mantle for long periods of time (> 1 Ga) (e.g., White, 1985; Zindler and Hart, 1986; Weaver, 1991). Isotope systematics of oceanic basalts reveal at least five end-members. These are DM (depleted mantle), HIMU (high μ), two enriched mantle reservoirs (EM-1 and EM-2) and C. The latter type, however, is thought to be common to all oceanic basalts (Hanan and Graham, 1996). C is, in a general sense, comparable with PREMA (Prevalent mantle; Zindler and Hart, 1986), PHEM (Primitive helium mantle; Farley et al., 1992), and FOZO (Focal Zone; Hart et al., 1992). If we accept the premise that such distinct reservoirs or domains exist in the earth's mantle, then the important question would be how they have acquired their diverse geochemical signatures. It must be noted, however, that only a small portion of oceanic island basalts (OIBs) show extreme isotopic compositions which might be characteristic of an end-member; most OIBs define an isotopic range that reflects mixing including at least two end-members, in which C is found in almost all cases (e.g., Hanan and Graham, 1996).

Geochemical signatures of OIBs are of particular importance for understanding the nature of the mantle end-members, which, in turn, help us to understand the geochemical diversity observed in the Earth's mantle. This information acquired from our present knowledge on OIBs can be also useful for understanding the OIB-type geochemical signatures found in ancient tectonic suites, such as ophiolitic complexes, mélanges and subduction/accretion complexes (e.g., Volkova and Budanov, 1999; Saccani and Photiades, 2005; Sayit and Göncüoglu, 2009; Prendergast and Offler, 2012). Geochemical systematics of modern OIBs, therefore, carry important insights into geochemical characterization of the ancient OIB-type rocks and the nature of the mantle from which they have originated. Trace element systematics have been widely used to explain the petrogenesis of both modern and ancient mafic rocks (e.g., Hofmann and Jochum, 1996; Condie, 2005; Pfänder et al., 2007; Aldanmaz et al., 2008; Sayit et al., 2010). In this paper, I mainly focus on immobile trace element systematics of OIBs to shed light on the two main issues: 1) What are the trace element systematics of the melts with distinct end-member signatures?, 2) What can the trace element systematics of OIBs tell us about their genesis? Apart from these, I will also briefly mention how this information relates to the OIB-type rocks from ancient tectonic settings, such as those from the Tethyan realm.

SOME NOTES ON THE BEHAVIOR OF TRACE ELEMENTS

In contrast to isotopic ratios, which reflect the exact geochemical signature as the source region (e.g., Hofmann and Hart, 1978), trace element ratios can be fractionated by processes like partial melting, depending on the behavior of the element under consideration (e.g., Shaw, 2006). Ratios of highly incompatible trace elements are thought to reflect source signatures (e.g., Hofmann and Jochum, 1996), since the fractionation between these elements will be relatively small. In contrast, the ratio of a relatively incompatible element to a moderately compatible or compatible element will be sensitive to partial melting. In this case, fractionation would be inevitable except for large degrees of melting.

While the effects of post-magmatic processes (e.g., alteration and metamorphism) do not generally pose a big trouble

for the modern oceanic rocks, this is apparently not the case for the ancient analogues. It has been shown that elements of high ionic potential (e.g., HFSE and REE) are relatively immobile during secondary processes, whereas elements of low ionic potential (e.g., LILE except for Th) can be mobilized by aqueous fluids in such conditions (e.g., Pearce and Cann, 1973; Ludden et al., 1982; Staudigel and Hart, 1996; Johnson and Plank, 1999). Therefore, trace elements employed in the discussion are Zr, Nb, La, Th, Y and Yb, which are all fluid-immobile, resistant to some degree of alteration and metamorphism (e.g., Pearce and Cann, 1973; Pearce, 2008).

The order of compatibility for the elements used here, in peridotitic upper mantle conditions, is as follows (starting from more incompatible): Th > Nb > La > Zr > Y > Yb (e.g., Sun and McDonough, 1989). Therefore, a trace element pair like Th-Nb is expected to be largely source-related, whereas pairs like Nb/Y and La/Yb will be largely affected by partial melting, especially in the presence of residual garnet (e.g., McKenzie and O'Nions, 1991). It must be noted, however, that this partitioning behavior would be different in the presence of distinct lithologies, such as eclogite/pyroxenite, owing to the compositional change in the mineral phases as well as introduction of some accessory ones (e.g., van Westrenen et al., 1999; Klemme et al., 2005; Pfänder et al., 2007).

METHOD

To examine the trace element systematics of the end-members, a dataset using the GEOROC database (http://georoc.mpch-mainz.gwdg.de/georoc/) was compiled, including 16 oceanic islands (Hawaii, Cook-Austral, Kerguelen, Iceland, Reunion, Canary, Samoan, Society, Azores, Marquesas, Tristan Da Cunha, Comoros, Cape Verde, Galapagos, Madeira, St. Helena). The database was accessed in 2012. All the samples are represented by basaltic extrusives except for two doleritic samples from Mangaia (Austral-Cook). Only the samples with greater than 7% MgO were used in the study in order to minimize the effect of fractional crystallization. Since the discussion and the modeling are mainly based on Th, Nb, La and Zr, only the samples including these four elements at the same time were used in order to make the plots comparable in terms of the samples used, thus avoiding to plot distinct samples as much as possible.

Since the end-members have been defined on the basis of the isotopes, I separated the OIB samples into their respective end-members based on $^{87}Sr/^{86}Sr$, $^{143}Nd/^{144}Nd$ and $^{206}Pb/^{204}Pb$ ratios. The selection were performed on the following scheme: EM-1: ($^{87}Sr/^{86}Sr > 0.7035$; $^{206}Pb/^{204}Pb < 18.5$) and ($^{143}Nd/^{144}Nd < 0.5129$; $^{206}Pb/^{204}Pb < 18.5$), EM-2: ($^{87}Sr/^{86}Sr > 0.7040$; $18.5 < ^{206}Pb/^{204}Pb < 20.25$) and ($^{143}Nd/^{144}Nd < 0.5128$; $18.5 < ^{206}Pb/^{204}Pb < 20.25$), DM: ($^{87}Sr/^{86}Sr < 0.7035$; $^{143}Nd/^{144}Nd > 0.5130$; $^{206}Pb/^{204}Pb < 18.5$); C: ($0.7030 < ^{87}Sr/^{86}Sr < 0.7040$; $0.5128 < ^{143}Nd/^{144}Nd < 0.5130$; $18.5 < ^{206}Pb/^{204}Pb < 19.5$), HIMU ($^{206}Pb/^{204}Pb > 20.25$). Regarding $^{143}Nd/^{144}Nd$, the gap between DM and EM-1 was intentionally left in order to better monitor the DM component away from the effect of EM-1. The final dataset was represented by about 700 samples in which the data population is composed of 9% DM, 39% EM-1, 27% EM-2, 19% EM-2, 6% HIMU.

RESULTS

Observations from trace element systematics

In terms of Zr/Nb, HIMU-type melts display exclusively low Zr/Nb values and they are confined in a narrow interval (Fig. 1 and Table 1); the values reflecting Zr/Nb ≤ 5 comprise 90% of the total variation. In contrast, very high Zr/Nb ratios are only shown by DM-type melts, and DM appears to be much more variable compared to HIMU. The very high Zr/Nb ratios are represented by Iceland in the dataset (Icelandic-type DM; Zr/Nb = 9.0-43.4), whereas the low Zr/Nb values observed within DM are represented by the Hawaiian samples (Hawaiian-type DM; Zr/Nb = 2.7-5.3). The relatively high values within EM-1 are displayed by a part of Hawaiian OIB (Hawaiian-type EM-1: Zr/Nb = 3.2-20.3) in which 87% of the population reflects Zr/Nb > 10 (Fig. 2). In contrast, the other EM-1 (non-Hawaiian-type EM-1) defines a range between 4.1-14.6 in which only 28% of the population reflects Zr/Nb > 10. Thus, there is a clear difference between the two groups. C-type melts appears to be partly similar to HIMU-type in terms of Zr/Nb, displaying a restricted range displaced towards low values (Fig. 1 and Table 1; Zr/Nb ≤ 5 makes up 65% of the total variation). Some of the C-type melts extend to a larger Zr/Nb range, approaching to ~15, though these samples are not abundant (Zr/Nb > 10 comprise only 5% of the total variation) (Fig. 1 and Table 1). Towards EM-2, EM-1 and DM, higher Zr/Nb ratios become more frequent. While HIMU and C comprise most of the Zr/Nb population for the values ≤ 5 (90% and 65%, respectively), EM-2 is largely concentrated within 5 < Zr/Nb ≤ 10 (59%). Although DM comprises 55% of the variation within 10 < Zr/Nb ≤ 20, it still has 19% population for values > 20.

In terms of La/Nb, HIMU-type melts similarly display a limited range, consisting of 95% of its population within La/Nb ≤ 0.8. (Fig. 1 and Table 1). In contrast to HIMU, C and EM-2 display more extensive compositional ranges. Considering values of La/Nb ≤ 0.8 and 0.8 < La/Nb ≤ 1.0; C comprises a population of 66% and 28%, whereas EM-2 consists of 50% and 43%. EM-2 also has an 8% population for La/Nb > 1. DM and EM-1 also display extensive spectra, but they cluster towards high La/Nb values. DM has a 57% population for 0.8 < La/Nb ≤ 1.0 and 18% for La/Nb > 1. EM-1 shows the highest La/Nb ratios and comprises 27% population for La/Nb > 1. It must be noted that the Hawaiian-type EM-1 defines a steeper slope in Zr/Nb-La/Nb space than other EM-1, also extending towards higher values (Fig. 2). Thus, it seems that at least a part of Hawaiian OIB shows some distinct characteristics within EM-1 and among all the others.

In terms of Th/Nb, HIMU-type melts are observed to have a restricted range (Fig. 1 and Table 1); 72% of the total variation is found within 0.06 < Th/Nb ≤ 0.08. At the low Th/Nb side, C, EM-1 and DM display relatively similar characteristics; they all extend to lower Th/Nb than HIMU and EM-2 (for the values ≤ 0.06, C, EM-1 and DM consists of 20%, 23%, 48%, respectively). At the high Th/Nb side, however, C and EM-2 display significant population compared to DM, EM-1 and HIMU (for values > 0.08, C and EM-2 reflects 35%, 70%, respectively, whereas DM, EM-1and HIMU displays 13%, 17%, 23%, respectively). As seen from these values, the high end of EM-2 is especially striking with 70% of the population being greater than 0.08. It is noteworthy that Hawaiian-type EM-1 does not show high Th/Nb characteristics; nearly all the population (97%)

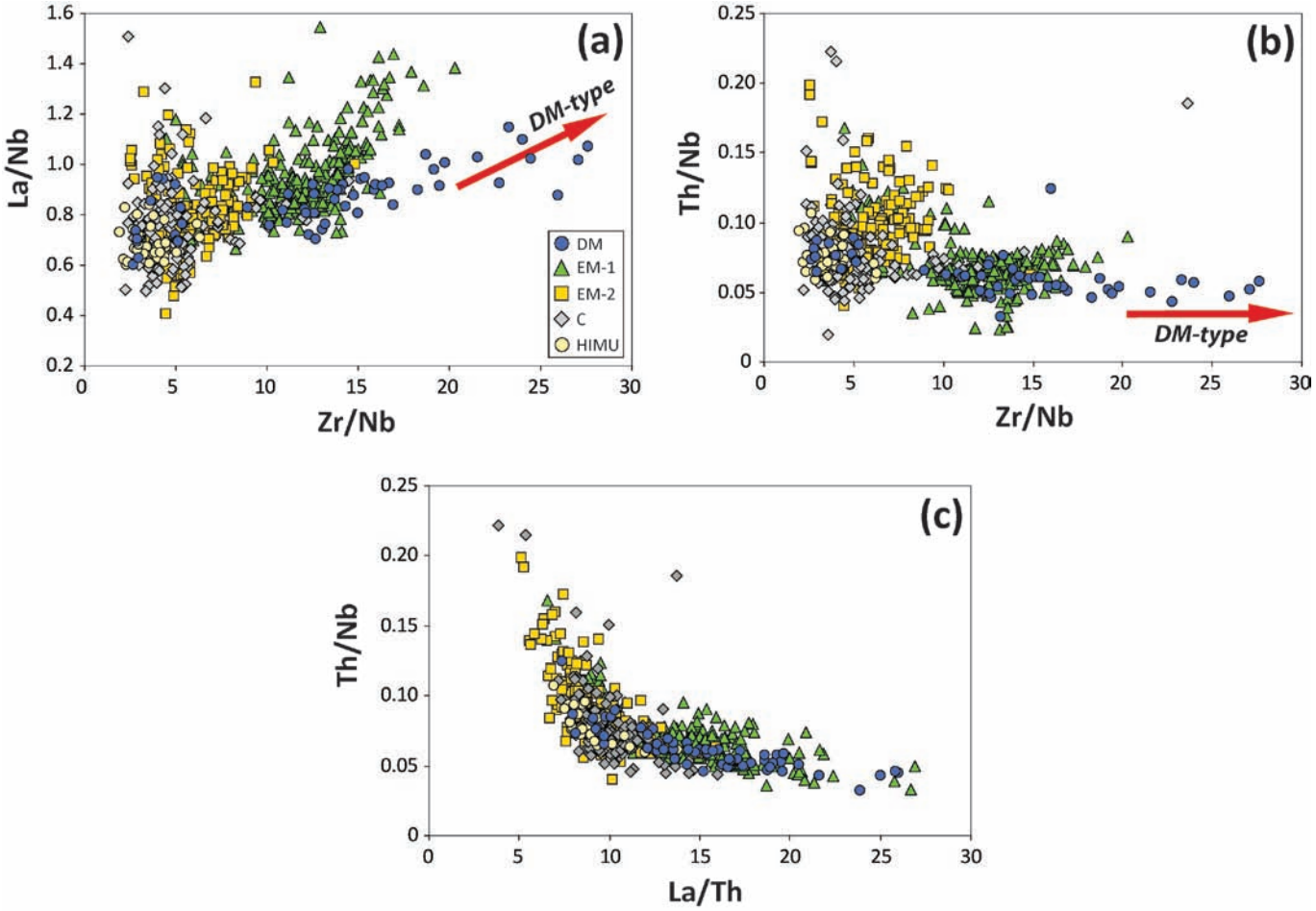

Fig. 1 - Trace element ratio-ratio plots.

Table 1 - Frequency distribution of the end-members for some trace element ratios.

Th/Nb					
Range	**DM**	**EM-1**	**EM-2**	**C**	**HIMU**
0.00-0.06	48.4	23.4	3.6	19.9	5.1
0.06-0.08	38.7	60.1	26.4	45.6	71.8
>0.08	12.9	16.5	69.9	34.6	23.1

Zr/Nb					
Range	**DM**	**EM-1**	**EM-2**	**C**	**HIMU**
0-5	14.5	2.9	39.4	64.7	89.7
5-10	11.3	21.2	59.1	30.1	10.3
10-20	54.8	75.5	1.6	4.4	0.0
>20	19.4	0.4	0.0	0.7	0.0

La/Nb					
Range	**DM**	**EM-1**	**EM-2**	**C**	**HIMU**
0-0.8	25.8	13.6	49.7	66.2	94.9
0.8-1	56.5	59.7	42.5	27.9	5.1
>1	17.7	26.7	7.8	5.9	0.0

La/Th					
Range	**DM**	**EM-1**	**EM-2**	**C**	**HIMU**
0-10	21.0	12.8	83.4	53.7	84.6
10-15	30.6	52.7	16.1	44.1	15.4
>15	48.4	34.4	0.5	2.2	0.0

The numbers are in terms of percent (%), which denotes the percentage of the population of a trace element ratio for a given end-member.

are confined within Th/Nb ≤ 0.08, whereas non-Hawaiian-type EM-1 reflects 76% population for Th/Nb > 0.08 (Fig. 2). Thus, Hawaiian-type EM-1 still appears to be distinct relative to the rest of EM-1.

In terms of La/Th, compositional range of the HIMU-type melts seems to be limited for La/Th ≤ 10 (85% is constrained within this interval) (Fig. 1 and Table 1). EM-2 and, to a lesser extent C, are also observed to concentrate largely for the values ≤ 10 (83% and 54%, respectively). EM-1 and DM, on the other hand, reflect extensive population for La/Th > 10 (87% and 79% respectively). It must be noted, however, that high La/Th ratios observed in EM-1 mostly comes from by Hawaiian OIB; the values with La/Th > 10 comprise 100% of the variation. Non-Hawaiian-type EM-1, however, includes only 32% population for La/Th > 10 (Fig. 2).

Correlations with $^{87}Sr/^{86}Sr$, $^{143}Nd/^{144}Nd$, $^{206}Pb/^{204}Pb$

When Th/Nb is plotted against $^{143}Nd/^{144}Nd$, no clear trend is observed except for EM-1 samples for which Th/Nb generally increases with decreasing $^{143}Nd/^{144}Nd$ (Fig. 3). This correlation is better defined with non-Hawaiian-type EM-1 (not shown). All type of end-members, however, display largely variable Th/Nb ratios for a given $^{143}Nd/^{144}Nd$. When La/Th is plotted against $^{143}Nd/^{144}Nd$, one trend seems to be sub-vertical, which is defined by EM-2; this trend goes towards very unradiogenic values. Some Hawaiian-type EM-1 reflect decreasing $^{143}Nd/^{144}Nd$ with increasing La/Th. However, non-Hawaiian-type EM-1 appears to be completely different; they largely reflect lower $^{143}Nd/^{144}Nd$ with decreasing La/Th. It is therefore noteworthy that EM-1 is observed to reflect two separate trends, a result also deduced from trace element ratio plots. Another feature to be noted from the plot is that EM-1- and DM-type melts show significant ranges in La/Th for a given $^{143}Nd/^{144}Nd$. La/Nb seems rather uncorrelated with $^{143}Nd/^{144}Nd$ (Fig. 3).

When Th/Nb, La/Nb and La/Th are plotted against $^{87}Sr/^{86}Sr$, somewhat similar relationships are observed. Th/Nb displays a broad positive trend with $^{87}Sr/^{86}Sr$ in EM-1, in which non-Hawaiian-type EM-1 defines a better correlation (Fig. 4). The distinctions, however, become more clear when La/Th is considered (Fig. 4). DM displays a gentle negative slope, whereas EM-2 reflects an extensive range of $^{87}Sr/^{86}Sr$ in relatively constant La/Th. Similar to those seen in the previous plots, EM-1 show two distinct trends; Hawaiian-type EM-1 appears to be more scattered, though some attain radiogenic Sr isotopic values with increasing La/Th, whereas non-Hawaiian-type EM-1 follows the EM-2 trend. In terms of La/Nb, some Hawaiian-type EM-1 reflects

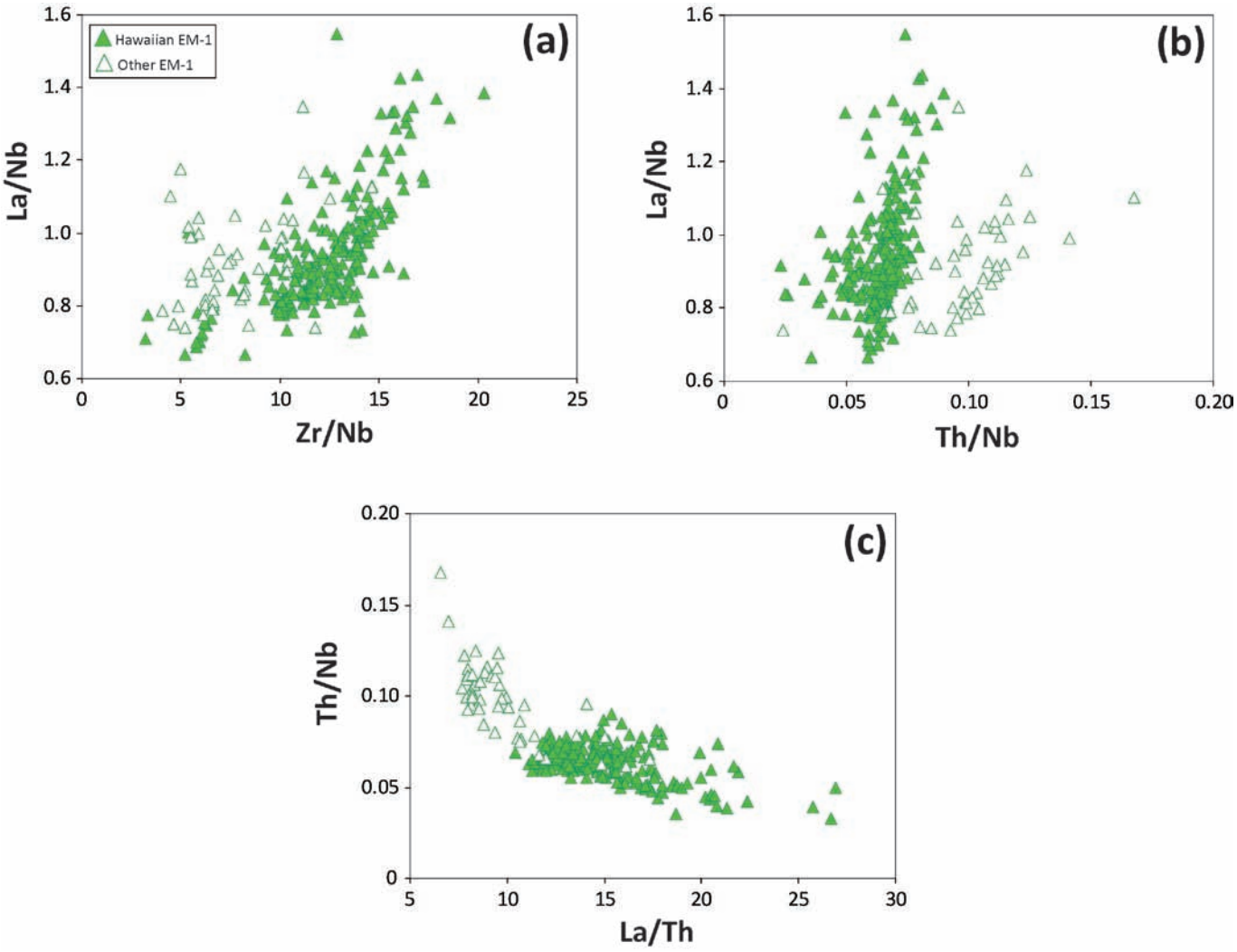

Fig. 2 - Trace element ratio plots, comparing Hawaiian-type EM-1 and other EM-1.

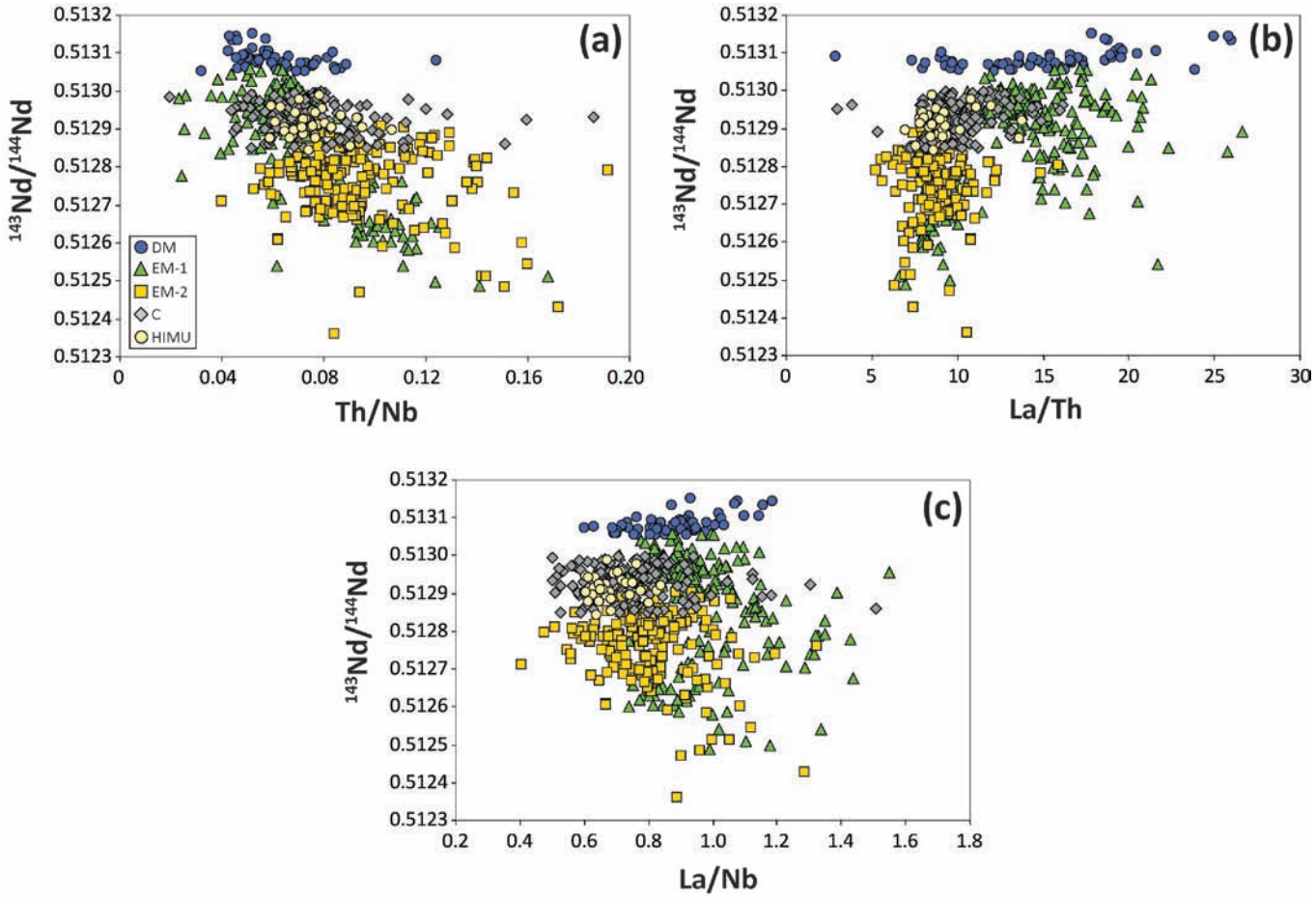

Fig. 3 - Plots of incompatible element ratios vs $^{143}Nd/^{144}Nd$.

a positive correlation. $^{206}Pb/^{204}Pb$ does not display any meaningful relationship with La/Nb, Th/Nb and La/Th. All end-member signatures span variable trace element ratios in a given $^{206}Pb/^{204}Pb$.

Regarding melting-sensitive ratios, Icelandic-type DM melts exhibit an inverse correlation in La/Yb vs. $^{143}Nd/^{144}Nd$ until a value of ~ 1.5 is attained (Fig. 5), then the trend becomes horizontal, spanning the relatively same isotopic value. Hawaiian-type DM follows this horizontal trend, displaying very large La/Yb spectrum for a given $^{143}Nd/^{144}Nd$. EM-2-type melts show a broad negative correlation, trending towards a component with high La/Yb, but low $^{143}Nd/^{144}Nd$. Similar to the previous plots, EM-1 appears as two distinct clusters. Hawaiian-type EM-1 shows a steep trend at a relatively constant La/Yb. The other EM-1-type melts follow a somewhat similar path first; however, they attain higher La/Yb ratios with decreasing $^{143}Nd/^{144}Nd$. In this plot, C and HIMU show no apparent correlation, reflecting large La/Yb spectra for a given $^{143}Nd/^{144}Nd$. Nb/Y also displays a similar relationship to La/Yb (Fig. 5). In contrast to some well-defined trends observed vs. $^{143}Nd/^{144}Nd$, the melting-sensitive ratios appear to be less correlated or uncorrelated with Sr and Pb isotopes.

DISCUSSION

Trace element characteristics of the end-members

Based on the results above, the first feature to be noted is that mantle end-member signatures cannot be clearly discriminated on the basis of trace element ratios. Different end-member signatures appear to overlap each other at varying extents (Fig. 1 and Table 1) in spite of the compatibility difference between trace elements used in the pair. Thus, it is not possible to say, for some intervals, that a specific trace element ratio reflects signatures that are specific to an end-member. At some intervals, however, some of the end-members become more dominant relative to others, such as DM with increasing Zr/Nb or EM-2 with increasing Th/Nb. The extensive variations in the source-related ratios, even within the same species, are also noteworthy (Fig. 1). Another important point is that although C represents the common region in isotopic spaces, on which the other end-members converge (e.g., Hanan and Graham, 1996), no such relation is observed in terms of trace elements.

Identification of possible processes and source materials

It is observed from the plots that mantle end-members reflect extensive ranges in terms of trace element ratios, except for HIMU being relatively limited. This situation also exists for very incompatible element ratios. The critical question would be: how can variable source-related trace element ratios reflecting similar isotopic characteristics be produced? Resolving this problem will be also essential for understanding of the presence of distinct isotopic signatures reflecting similar source-related ratios, since such ratios are generally thought to reflect differences in isotopic characteristics

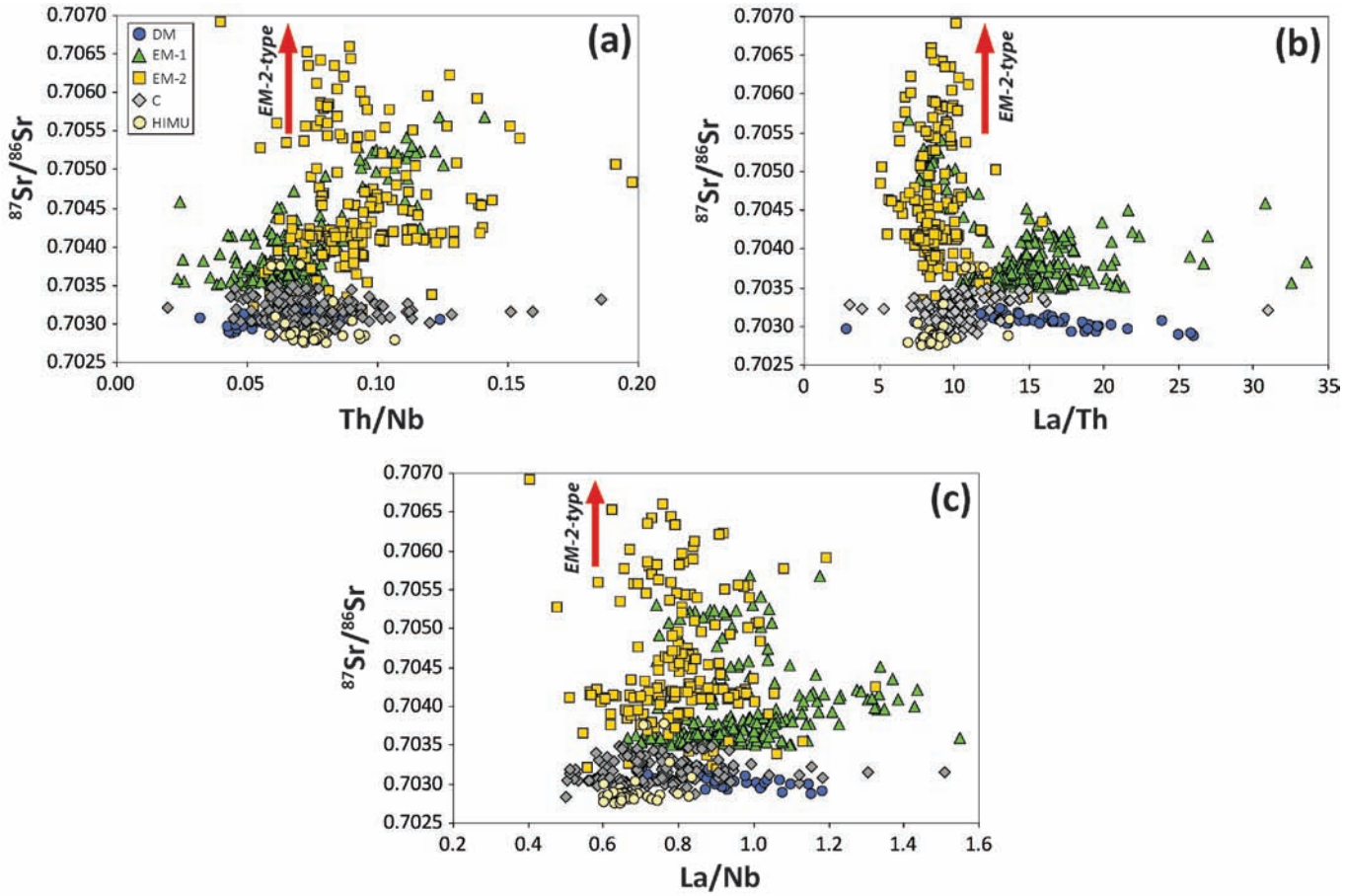

Fig. 4 - Plots of incompatible trace element ratios vs $^{87}Sr/^{86}Sr$.

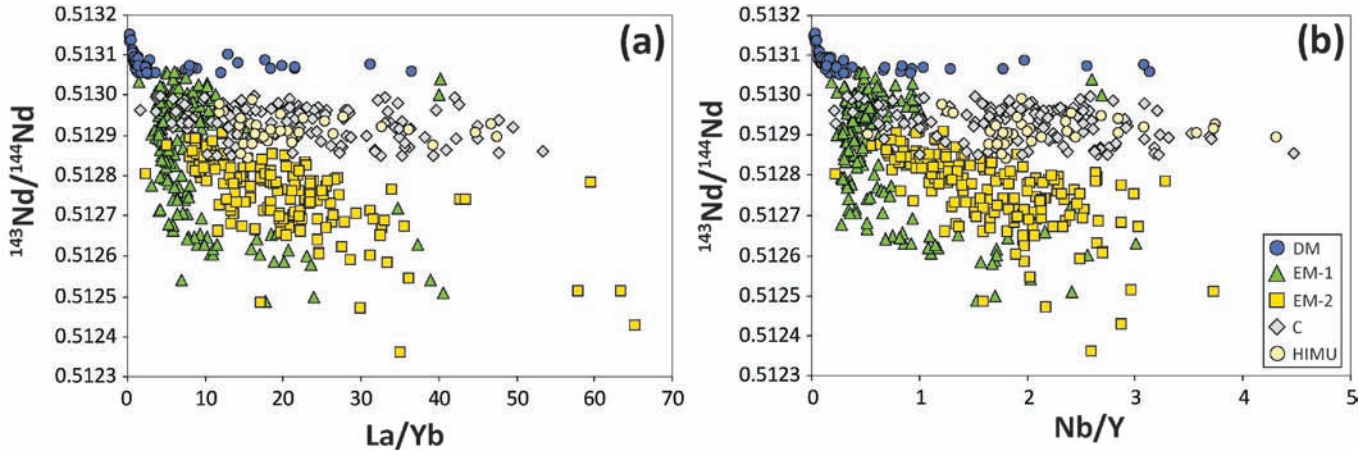

Fig. 5 - Plots of melting-sensitive trace element ratios vs $^{143}Nd/^{144}Nd$.

(e.g., Weaver, 1991). It is obvious that partial melting of a single homogeneous source cannot produce the observed variations, so another explanation is required. Processes, such as source mixing and melt mixing can create variable trace element and isotopic compositions. Partial melting of a single, but heterogeneous source, accompanied by melt mixing is also able to produce melts with distinct geochemical characteristics (e.g., Morgan, 1999; Ito and Mahoney, 2005).

The mantle is suggested to consist of enriched, small-scale heterogeneities in the form of veins and streaks embedded in a depleted matrix (e.g., Zindler et al., 1984; Allègre and Turcotte, 1986; Morgan and Morgan, 1999). This idea is supported by the existence of enriched MORBs (E-MORB) formed away from mantle plumes (e.g., Niu et al., 1999; Donnelly et al., 2004). One way to create these small-scale heterogeneities would be remixing of recycled oceanic crust as eclogitic/pyroxenitic bands, leading to a marble-cake structure (Allègre and Turcotte, 1986). In fact, such lithological heterogeneity is evidenced from the portions of

lithospheric mantle preserved in peridotitic massifs (e.g., Suen and Frey, 1987; Bodinier, 1988; Pearson et al., 1993; Fabriès et al., 1998; Montanini et al., 2012). Alternatively, heterogeneous mantle domains can also be formed by metasomatic processes (e.g., Niu and O'Hara, 2003; Pilet et al., 2005; Workman et al., 2004). Niu and O'Hara (2003) suggested that in oceanic lithosphere such domains can be generated by infiltration of volatile-enriched, low-degree melts originating from low velocity layer (LVZ) into the lithospheric mantle. These incompatible element-enriched melts, when freeze, may be preserved as pyroxenitic lithologies. The important feature regarding such heterogeneous source regions is that pyroxenitic/eclogitic lithologies have lower melting temperatures compared to anhydrous peridotite, so pyroxenitic/eclogitic lithologies can start melting before peridotite does (e.g., Hirschmann and Stolper, 1996; Pertermann and Hirschmann, 2003).

Trace element modeling

In order to place some constraints on the possible processes and mantle materials that may have contributed to the heterogeneity observed in OIBs, a ratio-based trace element modeling approach has been performed, taking into account both peridotitic and pyroxenitic/eclogitic lithologies. Before moving into the modeling, the effects of partition coefficients (D) and mineralogy on the calculated melting arrays will be briefly discussed.

The shape of the modeled melting curves depends on the D values as well as on the mineralogical and chemical source composition. The D values employed for the calculations are given in Table 2 (they will be called "the present D set" hereafter). During shallow mantle melting, olivine (ol) has very low D for the trace elements used here, so its effect on partitioning the elemental ratios is very small. However, clinopyroxene (cpx) and garnet (grt) and, to a lesser extent, orthopyroxene (opx) can alter these ratios, depending on their affinity for the elements considered. Based on the present D set, melting of a garnet lherzolitic source with a source mode 0.60 ol: 0.21 opx: 0.14 cpx: 0.05 grt gives bulk $D_{Th/Nb} = 0.6$ and $D_{La/Nb} = 3.7$. Thus, incompatible elements are in the order of incompatibility Th > Nb > La. While Th is more incompatible than Nb on the basis of a number of published D values (e.g., Hawkesworth et al., 1993; Bedard, 1994; Salters and Longhi, 1999; Salters et al., 2002), the relative compatibility between La and Nb may differ in some circumstances; La can become more incompatible than Nb. For example, the experimental results of Salters and Longhi (1999) and Salters et al. (2002) report relatively low $D_{La/Nb}$ values for cpx (1.4 and 0.92, respectively. Since D_{La} is not reported in these studies, D_{La} was calculated from D_{Ce}, assuming $D_{La/Ce} = 0.6$). This, in turn, results in bulk $D_{La/Nb}$ values lower than unity, meaning that La is more incompatible than Nb.

We cannot expect the mantle to be a mineralogically homogeneous entity. The change in modal mineralogy would in turn affect the bulk D values. For example, regarding a grt-peridotitic lithology, cpx/grt ratio can play an important role in controlling La/Nb ratio of the melt. This is because Nb is more compatible than La in garnet, whereas this case is reversed in the case of cpx. The increase in cpx/grt ratio tends to decrease the La/Nb ratio in the melt due to higher $D_{La/Nb}$ of cpx relative to grt (e.g., Johnson, 1998; Salters and Longhi, 1999). The effect of mineralogy becomes even greater when the lithology changes, since there is a compositional change in the mineralogy due to introduction of new minerals. Eclogites and pyroxenites can be generally regarded as bimineralic lithologies consisting of cpx and grt. Since the composition of these minerals is different than those in lherzolitic lithologies, this will result in distinct partitioning behavior of elements (e.g., van Westrenen et al., 1999; Klemme et al., 2002).

Discussion of modeling results

The geochemical modeling suggests that a peridotitic, depleted-DMM-like (D-DMM) lithology is required in the genesis of DM-type melts (Fig. 6a). Such material is especially needed to explain the very high Zr/Nb ratios of the Icelandic-type DM, since an enriched component cannot create such signatures along with low Zr and Nb abundances. This depleted peridotite is also capable of generating high La/Nb (> 1) and La/Th ratios (> 20) at high Zr/Nb and low La/Yb, thus making it an appropriate material for the DM genesis. Although melting of eclogitic N-MORB-type oceanic crust can produce high Zr/Nb ratios at large melt fractions, which encompass a large portion of the DM-type melts, it cannot explain the very high Zr/Nb ratios (> 35) (Fig. 6a).

Table 2 - Partition coefficients used in the melt modeling.

Peridotite Melting										
	La	ref	Yb	ref	Zr	ref	Nb	ref	Th	ref
oli	0.0004	1	0.0015	1	0.001	3	0.0001	2	0.00005	5
opx	0.0020	1	0.0490	1	0.0210	3	0.0030	2	0.0030	6
cpx	0.054	1	0.280	1	0.1600	3	0.0077	4	0.0036	6
grt	0.0010	2	4.0300	1	0.5000	3	0.0100	2	0.0020	6
spi	0.0006	2	0.0045	2	0.0700	2	0.0100	2	0.0010	7

Eclogite Melting										
	La	ref	Yb	ref	Zr	ref	Nb	ref	Th	ref
cpx	0.0339	1	0.5985	1	0.093	1	0.021	1	0.007	1
grt	0.0008	1	7.5050	1	0.400	1	0.008	1	0.0015	1

For peridotite melting, (1) McKenzie and O'Nions (1991), (2) Kelemen et al. (1993), (3) Shaw (2006), (4) Hart and Dunn (1993), (5) Salters et al. (2002), (6) Blundy and Wood (2003), (7) Hawkesworth et al. (1993). For eclogite melting, (1) Klemme et al. (2002). Since D_{Yb} is not reported in this study, it was calculated from D_{Lu}, assuming Yb/Lu = 0.95 (for both cpx and grt).

While a depleted peridotitic material is essential for explaining the depleted trace element characteristics of the DM-type melts, this material alone is clearly insufficient in explaining the entire elemental variation reflected by the DM clan and the other type of OIBs. This situation especially becomes evident owing to the presence of moderate/high Th/Nb ratios (Fig. 1 and Table 1), which cannot simply be obtained by melting a depleted peridotite. Instead, a peridotitic lithology having enriched-DMM-type (E-DMM) composition can create relatively enriched Th/Nb signatures (Fig. 6a). Although incorporation of melts derived from such material is able to explain the Th/Nb variation to some extent, it cannot account for the existence of higher values (Fig. 6a). In addition, some elemental systematics, such as Th/Nb-La/Nb and Th/Nb-La/Yb, still require additional material(s), since mixing of D-DMM- and E-DMM-type peridotitic melts fails to explain the entire compositional heterogeneity.

One solution to this problem would be involvement of recycled oceanic crust. Eclogitic lithologies are capable of partitioning Th from Nb (based on the present D set) and can produce high Th/Nb signatures at small melt fractions. On the basis of the modeling, melting of an eclogitic material with N-MORB-type composition actually explain the compositional variation observed in the DM-type melts (Fig. 6). Therefore, mixing of melts derived from three distinct lithologies, including a depleted peridotite (with D-DMM-like composition), a relatively enriched peridotite (with E-DMM-like composition) and an N-MORB-type eclogite (devoid of sediment) can fully explain the elemental systematics of the DM-type melts. Involvement of these materials is also in agreement with the depleted isotopic nature of the DM-type melts.

The modeling indicates that eclogitic N-MORB-type oceanic crust may have also been involved in the genesis of HIMU-type samples (Fig. 6b). Mixing of melts derived from oceanic crust and those from E-DMM-type peridotite appear to generate compositions that encompass nearly the entire range of HIMU-type melts. Although this mixing scheme is able to generate a wide spectrum of melt compositions, the elemental systematics of EM-1-, EM-2- and C-type melts seem to require a somewhat different material(s) than an N-MORB-type oceanic crust, owing to their more variable trace element ratios as well as distinct isotopic signatures (Figs. 1-4).

Unlike upper (basaltic) oceanic crust, oceanic crust including also a gabbroic portion may show distinct trace element signatures, such as higher La/Nb ratio (e.g., Niu and O'Hara, 2003). The modeling results suggest that melts of such oceanic crust, if mixed with peridotitic melts, can create compositions similar to observed in C and HIMU (Fig. 6c). Apart from gabbroic lithologies, sediments may also affect the elemental budget of the oceanic crust. One of the most notable features of the sedimentary lithologies is their Th-enriched nature, which enables them to develop high Th/Nb ratios (e.g., Plank and Langmuir, 1998). Sediments are thought to be recycled into mantle on top of the oceanic crust. During subduction, the uppermost part of oceanic slab is dehydrated and partially melted, thus losing some of its trace element content (e.g., Tatsumi, 1989; Pearce and Peate, 1995; Class et al., 2000). These "processed" or "residual" slabs may reflect variable compositions on the basis of the nature of sediment cover and the extent of subduction-filter (e.g., Plank and Langmuir, 1998; Porter and White, 2009).

The modeling results show that melts derived from such residual slabs, when combined with melts of E-DMM-type peridotite, can produce compositions that can explain the variations observed in EM-1 and EM-2 (Fig. 6d, e). Since the sediment signature is not totally lost on the residual slabs, recycling of these materials still appear to impart distinct geochemical features, such as high Th/Nb. However, addition of even small amount of sediment can disturb the isotopic budget of the slab and develop distinct isotopic signatures with aging (e.g., Chauvel et al., 1992; Hemond et al., 1994; Stracke et al., 2003).

Nature of the end-members

The important point deduced from the modeling is that involvement of a peridotitic lithology is essential for the genesis of all kind of mantle end-member signatures. Eclogitic lithologies alone cannot explain the entire variation observed in OIBs (Fig. 6). Such a result appears to contradict with some of the existing models that propose recycled oceanic crust as a sole component in OIB genesis (e.g., Hofmann and White, 1982; Weaver, 1991; Christensen and Hofmann, 1994). One of the problems with the latter idea, however, is that melting of oceanic crust create melts whose MgO contents are not high enough to be involved as a single lithology in the genesis of OIBs (e.g., Niu and O'Hara, 2003; Sobolev et al., 2005; Kogiso and Hirschmann, 2006). Therefore, contribution from a peridotitic lithology is also needed to explain the occurrence of high-MgO primary melts. This result is also supported by the major element systematics of the OIBs (Jackson and Dasgupta, 2008).

Fig. 6 - Melt modeling OIBs. A) DM-type, B) HIMU-type, C) C-type, D) EM-1-type, E) EM-2-type. All peridotitic melting curves were modeled by non-modal batch melting, whereas eclogitic melting curves were modeled by modal-melting. Calculations were performed using the equations of Shaw (1970). "Grt" = garnet, "spl" = spinel, "RS" = residual slab, "OC" = bulk oceanic crust consisting of both basaltic and gabbroic crust. Melt curves are represented by thick solid lines, whereas mixing lines are represented by thin lines with black dots. For simplicity, only a limited number of mixing lines were shown. In order to show the effects of mixing, one group of plots includes mixing lines emerging from a specific peridotitic melt fraction, which join to several points on the eclogitic curve, whereas another group comprises several mixing lines derived from the peridotite, which converge on the eclogite. The numbers on the melting curves indicate the degree of melting. Grt-peridotite source mode was taken as 0.600 ol + 0.210 opx + 0.120 cpx + 0.070 grt, which melts in the proportions 0.010 ol + 0.040 opx + 0.500 cpx + 0.450 grt. Regarding spl-lherzolite, the source mode was assumed to be 0.575 ol + 0.257 opx + 0.144 cpx + 0.024 spi (Kostopoulos and Murton 1992), which melts in the proportions 0.020 ol + 0.080 opx + 0.75 cpx + 0.150 spi (Haase et al. 1997). For eclogite melting, source/melt modes were taken as 0.700 cpx + 0.300 grt. For modeling DM-type melts, the depleted source is represented by slightly modified depleted-DMM (D-DMM) composition of Workman and Hart (2005) such that La was decreased to 0.11 ppm, whereas Nb was increased to 0.095 ppm. Thus the modified D-DMM-like source has relatively lower La/Nb and La/Th with respect to the original. The modification produced a better match, especially regarding the depleted compositions (high Zr/Nb). The modified E-DMM composition represents E-DMM composition of Workman and Hart (2005), except that Nb concentration was increased to 0.3 ppm for EM-1 and HIMU and increased to 0.35 ppm for C and EM-2. For the modeling of EM-1- and EM-2-type melts, Tonga and Izu-Bonin residual slab compositions of Porter and White (2009) were used, respectively. In the case of Hawaiian-type EM-1, however, La concentration was increased to 7 ppm (indicated as "RS-1" as compared to "RS-2" used for non-Hawaiian EM-1). N-MORB composition representing basaltic crust is taken from Sun and McDonough (1989). Average bulk oceanic crust is taken from Niu and O'Hara (2003).

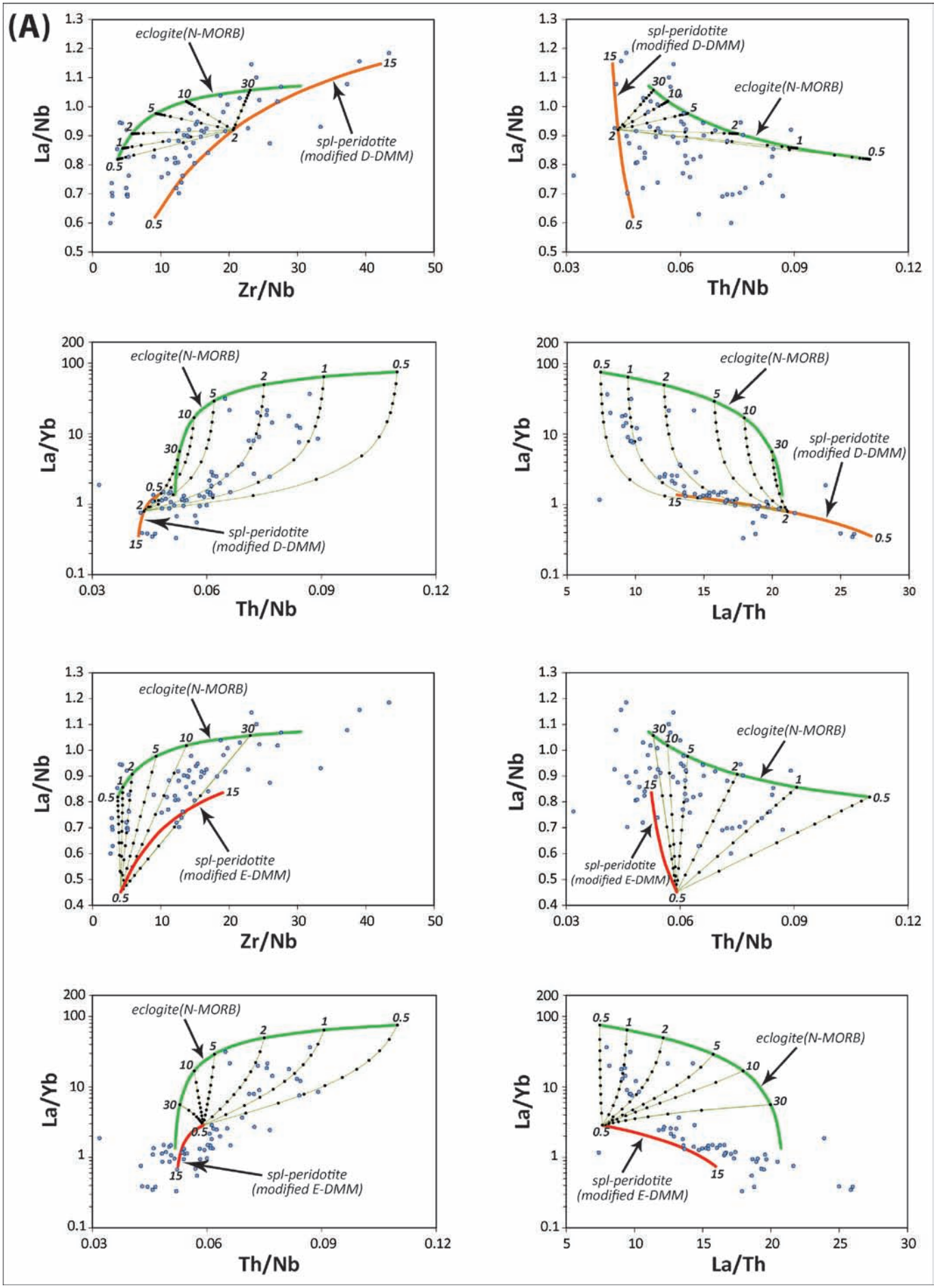
(A)
eclogite(N-MORB)
spl-peridotite
(modified D-DMM)
La/Nb
Zr/Nb
Th/Nb
La/Yb
La/Th
spl-peridotite
(modified E-DMM)

continued

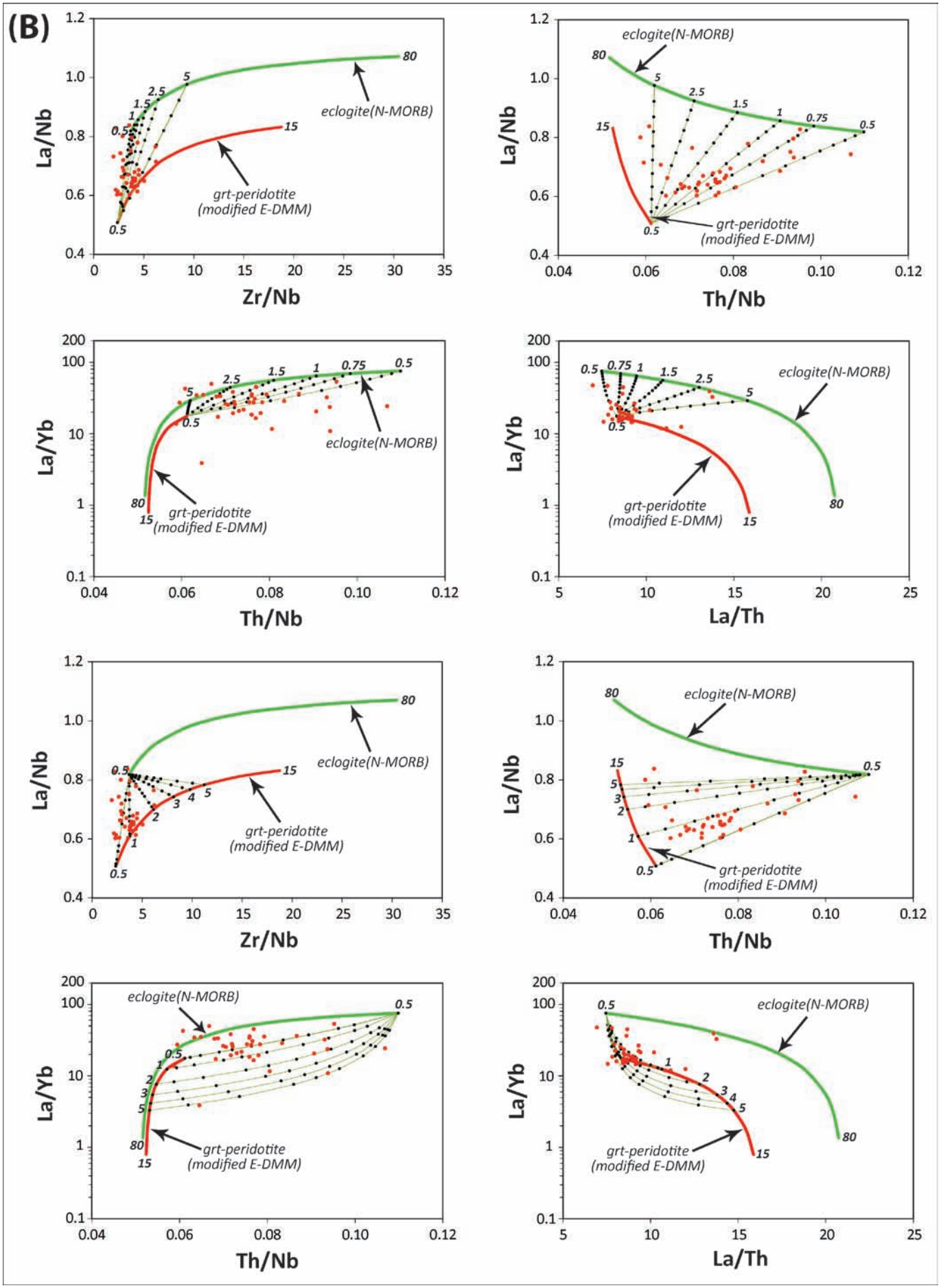
(B)
La/Nb
Zr/Nb
eclogite(N-MORB)
grt-peridotite
(modified E-DMM)
La/Nb
Th/Nb
eclogite(N-MORB)
grt-peridotite
(modified E-DMM)
La/Yb
Th/Nb
eclogite(N-MORB)
grt-peridotite
(modified E-DMM)
La/Yb
La/Th
eclogite(N-MORB)
grt-peridotite
(modified E-DMM)
La/Nb
Zr/Nb
eclogite(N-MORB)
grt-peridotite
(modified E-DMM)
La/Nb
Th/Nb
eclogite(N-MORB)
grt-peridotite
(modified E-DMM)
La/Yb
Th/Nb
eclogite(N-MORB)
grt-peridotite
(modified E-DMM)
La/Yb
La/Th
eclogite(N-MORB)
grt-peridotite
(modified E-DMM)

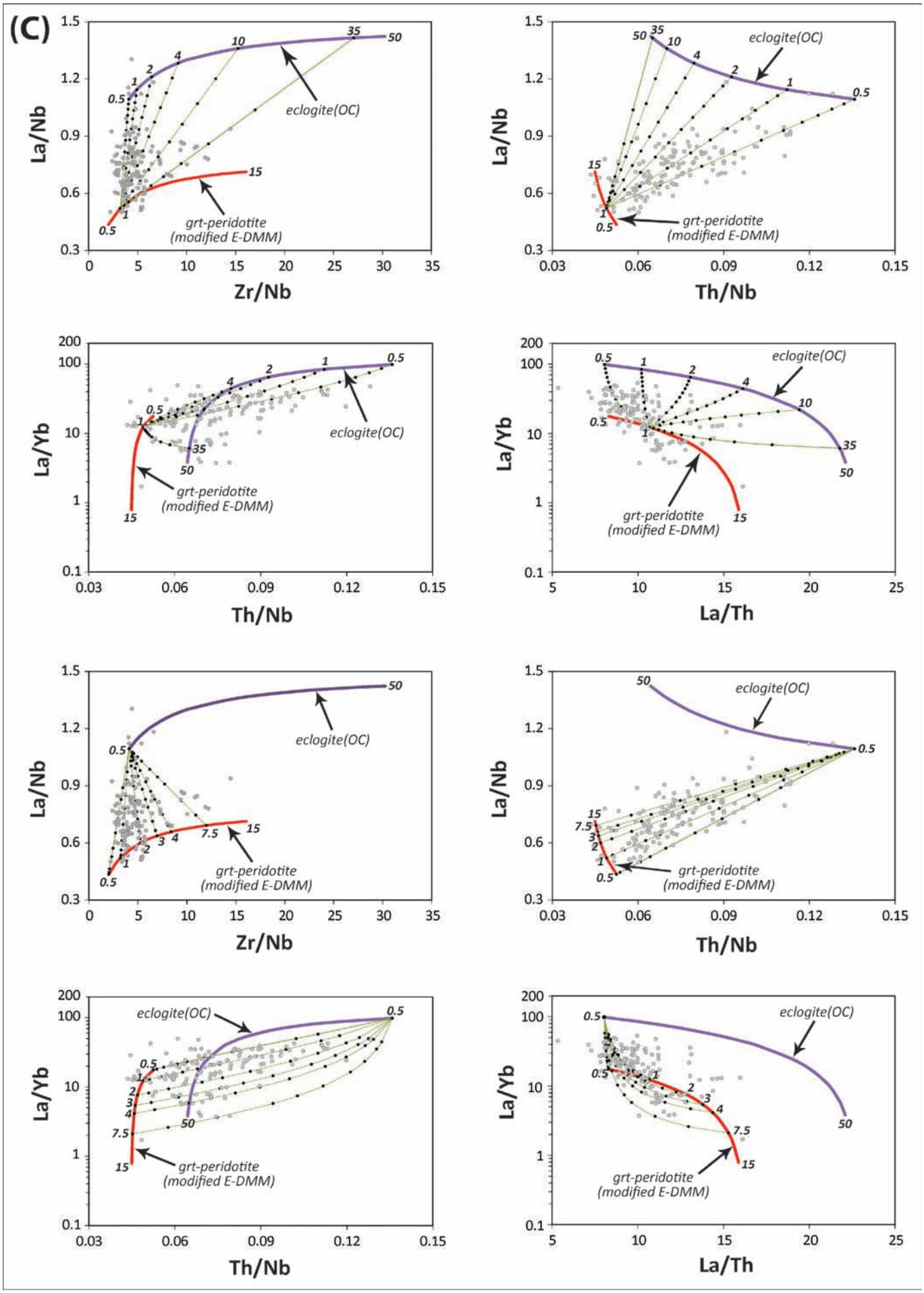
(C)
La/Nb
Zr/Nb
eclogite(OC)
grt-peridotite
(modified E-DMM)
La/Nb
Th/Nb
eclogite(OC)
grt-peridotite
(modified E-DMM)
La/Yb
Th/Nb
eclogite(OC)
grt-peridotite
(modified E-DMM)
La/Yb
La/Th
eclogite(OC)
grt-peridotite
(modified E-DMM)
La/Nb
Zr/Nb
eclogite(OC)
grt-peridotite
(modified E-DMM)
La/Nb
Th/Nb
eclogite(OC)
grt-peridotite
(modified E-DMM)
La/Yb
Th/Nb
eclogite(OC)
grt-peridotite
(modified E-DMM)
La/Yb
La/Th
eclogite(OC)
grt-peridotite
(modified E-DMM)

continued

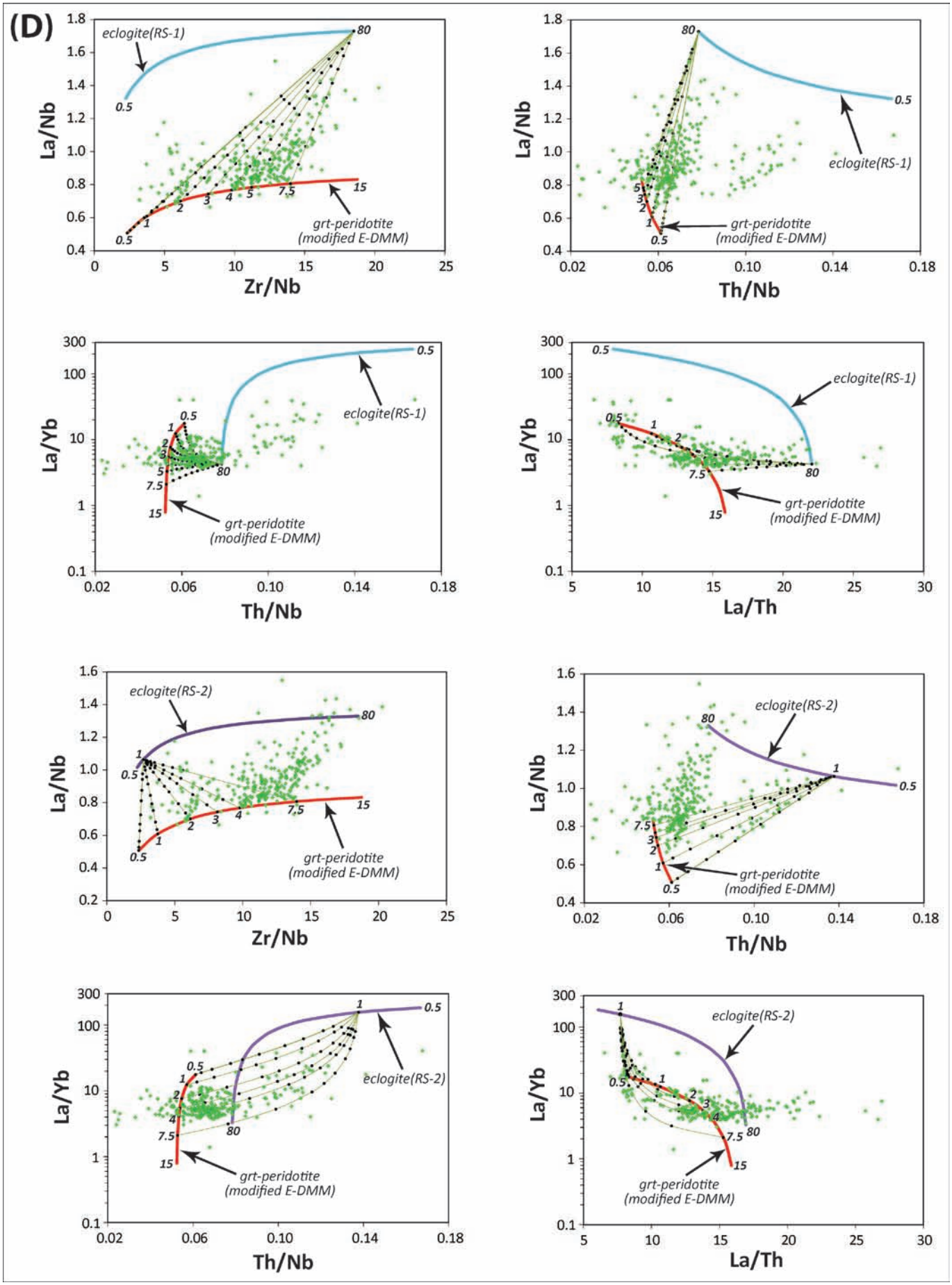
(D)
eclogite(RS-1)
grt-peridotite
(modified E-DMM)
La/Nb
Zr/Nb
Th/Nb
La/Yb
La/Th
eclogite(RS-2)

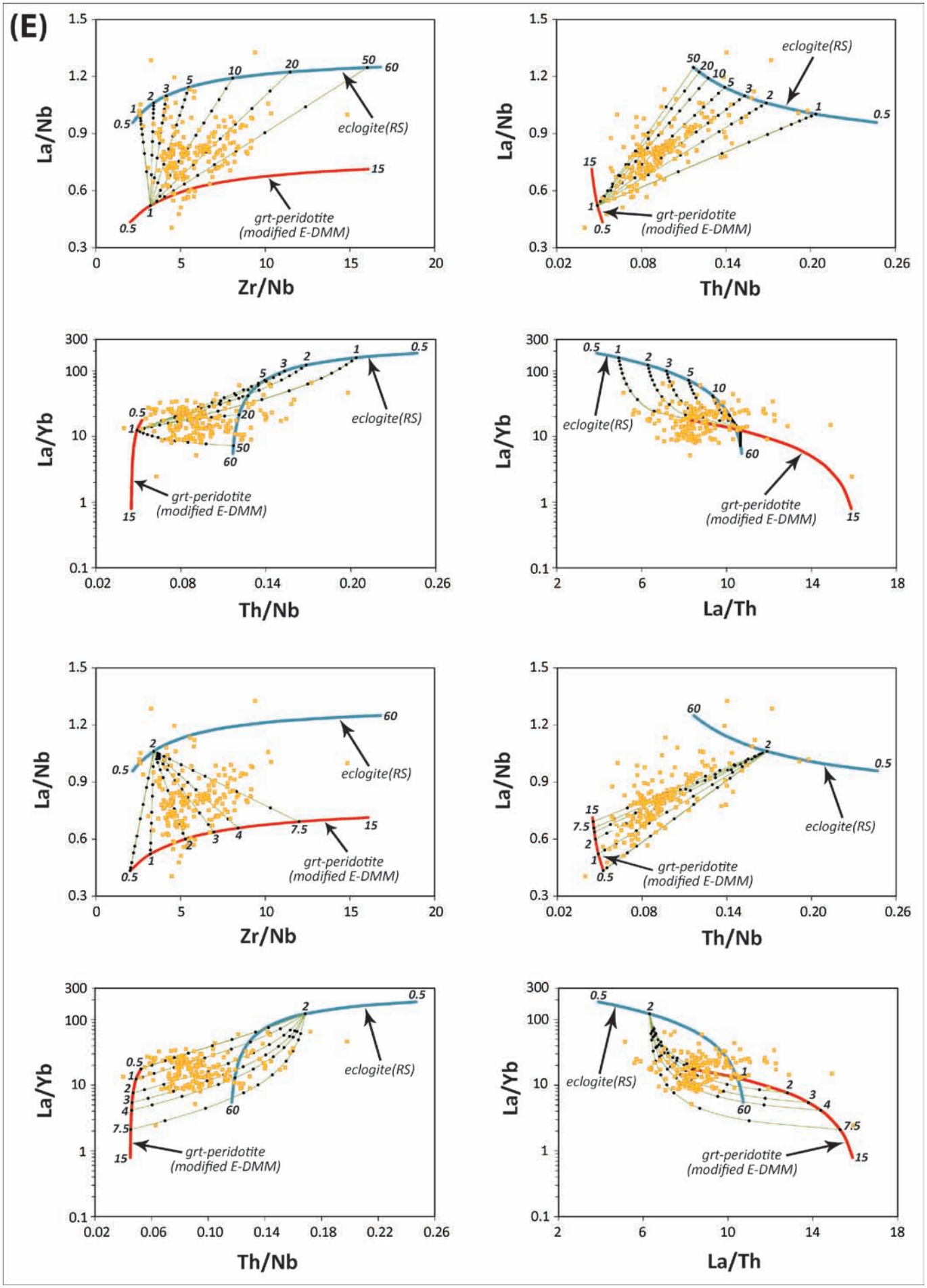
(E)
La/Nb
Zr/Nb
eclogite(RS)
grt-peridotite
(modified E-DMM)
La/Nb
Th/Nb
eclogite(RS)
grt-peridotite
(modified E-DMM)
La/Yb
Th/Nb
eclogite(RS)
grt-peridotite
(modified E-DMM)
La/Yb
La/Th
eclogite(RS)
grt-peridotite
(modified E-DMM)
La/Nb
Zr/Nb
eclogite(RS)
grt-peridotite
(modified E-DMM)
La/Nb
Th/Nb
eclogite(RS)
grt-peridotite
(modified E-DMM)
La/Yb
Th/Nb
eclogite(RS)
grt-peridotite
(modified E-DMM)
La/Yb
La/Th
eclogite(RS)
grt-peridotite
(modified E-DMM)

Recently, Sobolev et al. (2005) suggested an 'olivine-free' source for the genesis of Hawaiian shield-lavas. According to this model, eclogitic oceanic crust, which rises along with the plume, melts and reacts with the surrounding peridotite, creating a secondary/hybrid pyroxenite. Then, melts derived from this pyroxenitic lithology mixes in variable proportions with melts from unreacted peridotite, generating the final melt composition. Sobolev et al. (2007) proposed that this mechanism is also applicable to the genesis of MORBs, some LIPs as well as tholeiite-dominant OIBs, such as Iceland. It must be noted that although contribution from a pyroxenitic source is necessary, a peridotitic lithology is also needed in this model, thus in agreement with the result obtained in the present study.

Another point evidenced by the modeling is that mixing of melts derived from at least two distinct materials/components (of different composition) is needed to explain the entire compositional spectrum for a specific end-member. A solid evidence for this result comes from the significant variation of Th/Nb ratio whose fractionation is relatively small in peridotitic upper mantle conditions, which is shown on the plots (Fig. 6). As explained above, one of the materials involved in the OIB genesis should be of peridotitic mineralogy. The other material(s) involved in the mixing scheme can be another peridotite with a different composition (e.g., a peridotite with D-DMM-like composition and another with E-DMM-like composition) and/or eclogite.

The depleted isotopic nature of DM (high $^{143}Nd/^{144}Nd$, low $^{87}Sr/^{86}Sr$ and $^{206}Pb/^{204}Pb$; e.g.. Zindler and Hart, 1986) is in well agreement with the predominant involvement of a DMM-like and/or E-DMM-like peridotitic mantle source with/without basaltic oceanic crust. Sole involvement of an enriched component(s) cannot account for depleted isotopic characteristics. The highly depleted trace element ratios observed in the DM-type melts (very high Zr/Nb and high La/Nb) can be attributed to the significant contribution of the melts derived from a depleted, volatile-free peridotite (e.g., Ito and Mahoney, 2005). Less depleted trace element compositions, on the other hand, require involvement of relatively enriched peridotitic material and/or N-MORB-type oceanic crust (Fig. 6). In this regard, the enriched trace element characteristics of the Hawaiian-type DM can be explained by incorporation of small degree melt fractions derived from E-DMM-type peridotite and eclogite. The contribution of eclogitic/pyroxenitic lithologies to the genesis of OIBs with depleted isotopic characteristics is also in agreement with the other studies (e.g., Ito and Mahoney, 2005; Sobolev et al., 2007; Stracke and Bourdon, 2009). In addition to basaltic oceanic crust, minor contribution from gabbroic lower crust is also possible in the genesis of DM-type OIB. Major incorporation of gabbroic lower crust, however, does not seem very likely, since it would generate melts with high La/Nb ratios (Fig. 6).

On the basis of trace element systematics, an E-DMM-like peridotite appears to be a suitable source material not only for DM, but also for the other end-member types (i.e., EM-1, EM-2, HIMU and C). However, although E-DMM-type peridotite is able to explain the relatively depleted part of C, it is still too depleted to explain its isotopically enriched side as well as the extreme isotopic signatures of EM-1, EM-2 and HIMU. Then, the important question is how this peridotitic source can also generate isotopically enriched and extreme source signatures. The fact that DMM-like Th/Nb signatures is coupled with enriched and distinct isotopic characteristics may suggest that this peridotitic material has been metasomatized, and it is not a volatile-free peridotite. Dixon et al. (2002) showed that C/FOZO plumes are enriched in water (~ 0.08% H_2O), which clearly excludes a significant contribution from a volatile-free peridotite. This result, therefore, is in well-agreement with that acquired by this study, at least for the nature of C. The involvement of a metasomatized peridotite in creating EM-1-, EM-2- and HIMU-type signatures is perhaps not surprising. This is because C-type melts are involved in almost every mixture creating the OIBs (e.g., Hanan and Graham 1996), and the extreme compositions are only rarely found or yet to be found (e.g., Jackson et al. 2007). Therefore, involvement of a metasomatized peridotite seems to be suitable not only for the genesis of C-type melts, but also for the other types of end-member signatures.

Non-Hawaiian-type EM-1 and EM-2 signatures can be explained by entrainment of residual slabs, which carry some amount of sediment (Fig. 6d, e). This is also supported by dominantly high Th/Nb character of these end-members. As deduced from modeling, such material providing high Th/Nb and La/Nb can be created in the form of an eclogitic crust. Although both non-Hawaiian EM-1 and EM-2 are consistent with a sedimentary component, distinct isotopic characteristics of these two end-members suggest heterogeneous sedimentary lithologies (e.g., Weaver, 1991; Eisele et al., 2002). Regarding EM-2, the existence of Samoan lavas with very high $^{87}Sr/^{86}Sr$ ratios (up to 0.720469, Jackson et al., 2007) has placed a strong constraint on the involvement of recycled sediment in the genesis of this end-member. The importance of sediments in the genesis of OIBs is also evidenced by Nd-Hf isotopic systematics which requires a sedimentary component(s) to fully explain compositional variation observed in OIBs (Chauvel et al., 2008).

The generation of Hawaiian-type EM-1, on the other hand, requires a different explanation, as reflected by its distinct trace element systematics. The somewhat depleted elemental ratios (moderate Zr/Nb associated with high La/Nb and La/Th) compositions in Hawaiian-type EM-1 reflect isotopically enriched signatures. Therefore, although their trace element systematics seem compatible with a DMM-like, depleted component at the first glance, the enriched isotopic signatures are definitely not (e.g., Chen and Frey, 1985). This decoupling of trace element and isotopes may imply a relatively recent partial melting and/or melt extraction that has led to depletion in the source region (e.g., Frey and Rhodes, 1994). Alternatively, these signatures can be explained by involvement of recycled oceanic crust with gabbroic component (e.g., Sobolev et al., 2000; Gaffney et al., 2004). Melting of gabbroic lithologies can generate high Zr/Nb, La/Nb and La/Th signatures, which may be compatible with the nature of Hawaiian-type EM-1. However, the modeling results suggest that although a basaltic/gabbroic material can provide such geochemical characteristics, the mixing trends do not produce good fits on the plots (not shown). Instead, incorporation of a residual slab (including some amount of sediment) produces mixing lines that provide a better fit to the observed variation, if this residual slab is relatively enriched in La (Fig. 6d). If this is indeed the case, the difference between Hawaiian EM-1 and the rest of EM-1 can be explained in a way that the former type requires higher-degree melt fractions from a relatively La-enriched, eclogitic/pyroxenitic component.

Compared to EM-type melts, which require isotopically enriched components like sediment, C and HIMU are believed to reflect negligible contribution of such enriched

components in terms of recycling of oceanic crust (e.g., Weaver, 1991; Chauvel et al., 1992; Hemond et al., 1994; Woodhead, 1996; Stracke et al., 2005). In this sense, HIMU requires ancient oceanic crust devoid of sediment, while C may represent immature/young HIMU owing to its relatively depleted isotopic signatures (e.g., Weaver, 1991; Hanan and Graham, 1996; Stracke et al., 2005). However, majority of OIBs including the ones with HIMU-type characteristics are known to be silica-undersaturated, which contrast with the silica-saturated nature of N-MORB-type oceanic crust (e.g., Green et al., 1967; Kogiso et al., 2003; Jackson and Dasgupta, 2008). This fact, therefore, demands for another mechanism and/or material in the genesis of HIMU, which can generate silica-deficient signatures. One such material would be a silica-deficient pyroxenite, a lithology not uncommon in both xenoliths and peridotitic massifs (see Hirschmann et al., 2003). These authors have shown that silica-deficient garnet pyroxenite is able to produce some major element characteristics similar to found in silica-undersatured OIBs. Alternatively, a bimineralic eclogite can also create silica-poor melts, provided that the eclogite have previously experienced fractional removal of fluids or melts (Kogiso and Hirschmann, 2006). Therefore, recycled oceanic crust in the form of silica-deficient pyroxenite or processed eclogite can be a plausible source material in the genesis of HIMU as well as C.

The modeling indicates that a residual slab containing some amount of sediment is also possible (not shown). However, if sediment is involved in the genesis of C and HIMU, it should be probably very small, since addition of sediment will disturb the isotopic budget of the oceanic crust, leading to some extreme signatures with aging (e.g., Hemond et al., 1994; Stracke et al., 2003). Regarding C, an alternative solution would be that some sediment has been indeed involved, but it was relatively young so that it could not develop extreme isotopic signatures. It is also noteworthy that although C and HIMU may be somewhat related on the basis of their isotopic characteristics (e.g., Hanan and Graham, 1996; Stracke et al., 2003), trace element systematics suggest that they may have not evolved from exactly the same material(s) or that they have acquired distinct melt contributions from eclogitic and/or peridotitic lithologies. C-type melts displays a larger Th/Nb and La/Nb range than HIMU. The difference is especially clear in the case of La/Nb. On the basis of modeling, regarding the first option, a basaltic oceanic crust may have been involved in the generation of HIMU-type melts, while the entire oceanic crust (including also gabbros) may have associated with the origin of C-type melts (Fig. 6b, c). In contrast, in the case of the second option, the entire oceanic crust may have been involved in the generation of both types of melts. In this case, however, HIMU-type melts appear to receive less contribution from the eclogitic upper crust, i.e., peridotitic melts may be more dominant. The relatively homogeneous character of HIMU both in terms of trace and isotope systematics can be due to predominant tapping of melts derived from one lithological component or a portion within oceanic lithosphere.

As shown above, the presence of oceanic crust (± sediments) appears to be suitable for the creation of isotopically-enriched end-member signatures (i.e., C, EM-1, EM-2 and HIMU), though it cannot fully explain the trace element systematics alone. A peridotitic material, which is probably isotopically enriched and metasomatized, is also needed. Thus, the mantle source materials of the OIBs can be envisioned as fragments of "metasomatized oceanic lithosphere" consisting of both eclogitic and peridotitic lithologies. Metasomatism of the lithospheric part may occur via infiltration of volatile-rich fluids and/or melts that later freeze as pyroxenite (e.g., Niu and O'Hara, 2003; Workman et al., 2004). This process is thought to take place during generation and subsequent cooling of oceanic lithosphere at mid-ocean ridge setting. Such metasomatic process can also occur via involvement of a carbonated oceanic crust (e.g., Dasgupta et al., 2004; Jackson and Dasgupta, 2008). In this case, if carbonated eclogites exist as preserved lithologies, melts derived from these readily-fusible materials can metasomatize the peridotite at upper mantle conditions (Jackson and Dasgupta 2008). Alternatively, these lithologies can totally mix with each other, converting to a single, hybrid, volatile-rich peridotite (Jackson and Dasgupta, 2008). Metasomatism of oceanic lithosphere can also be achieved by "percolative fractional crystallization" as suggested by Pilet et al. (2005), in which melts derived from upper mantle infiltrate into lithospheric mantle. The distinctive feature of this model, however, is that the melt experiences modification through fractionation of accessory phases, such as apatite, rutile and ilmenite. Since these phases have distinct partitioning abilities, such process can create veins with variable Th/Nb, La/Nb and La/Th ratios, and develop variably enriched isotopic signatures with aging.

Further considerations

The geochemical modeling presented here shows that a peridotitic component is required in generation of all end-member types, which is a result also consistent with major element chemistry of OIBs (Jackson and Dasgupta, 2008). Furthermore, the peridotitic material involved in the generation of C, HIMU, EM-1 and EM-2 appears to be distinct from depleted DMM. The other components can be eclogitic/pyroxenitic oceanic crust with/without sediments. Therefore, it seems that the melts carrying distinct end-member signatures may have been inherited from similar settings, i.e., parts of oceanic lithosphere (crust + lithospheric mantle). Such a scenario would be consistent with the common idea for the genesis mantle plumes, i.e., recycling of the oceanic crust (Hofmann and White, 1982; White and Hofmann, 1982; Weaver, 1991).

Recent studies suggested that recycled oceanic crust alone is not a suitable source material to be involved in the genesis of OIBs (e.g., Niu and O'Hara, 2003; Collerson et al., 2010). Furthermore, experimental studies indicate that MORB-type oceanic crust remains denser at all depths below 720 km than the surrounding mantle (Hirose et al., 2005). Instead of oceanic crust, Niu and O'Hara (2003) suggested metasomatized oceanic lithospheric mantle, since mantle part of the lithosphere is of peridotitic composition (Mg-rich) that gives it positive buoyancy. Collerson et al. (2010), on the other hand, proposed carbonate-rich lower mantle melts and residues in the genesis of OIBs. If, however, the mantle part of the lithosphere remains attached to the oceanic crust subducted into the mantle, then oceanic crust (with its mantle part) can still rise in the form of plume (e.g., White, 2010). Therefore, it may seem more realistic to envision the recycling slabs as oceanic lithosphere (crust + lithospheric mantle) rather than only oceanic crust, especially due to density considerations.

Trace elements systematics suggests that C and the other types of melts may have derived from similar type of materials, i.e., fragments of oceanic lithosphere (crust plus man-

tle part). An important question would be what makes C special? How can this end-member be the common isotopic region, yet represented by a similar material? It has been shown that slabs may stagnate on the 660 km boundary (e.g., Fukao et al. 2009), but they eventually sink into lower mantle (e.g., Kellogg et al., 1999; Hirose et al., 2005). The ancient slabs, on the other hand, reside at the bottom of lower mantle. In this sense, the young, stagnant slabs (or the ones that have not reached the bottom of the lower mantle) can be thought to represent the common C material, since such slabs would be entrained by the plumes rising from the bottom (which contain ancient slabs characterizing the other enriched end-member signatures). However, there are no stagnant slabs occurring on top of the Pacific or African superplume (Fukao et al., 2001; Maruyama et al., 2007). The youngest slabs underlying Pacific OIBs are characterized by the Rodinian slabs (~ 750-1000 Ma), whereas the Atlantic OIBs are underlain by Gondwanan slabs (~ 200-600 Ma) (Maruyama et al., 2007). Although there is an apparent age difference between the slabs underlying Pacific and Atlantic OIBs, all types of end-member signatures are encountered in both oceanic domains. Therefore, this may suggest that generation of the C-type melts is probably related to distinct modification/metasomatism of a portion of oceanic lithosphere, which operates in a similar way in the fate of all the subducting slabs during their journey into the lower mantle or during mantle convection, rather than entrainment of some special slabs characterized by C-type signatures.

Some remarks on the ancient analogues: the Tethyan case

The OIB-type melts are not only generated in the present tectonic settings, but are also common to ancient tectonic suites. The relics of the oceanic lithosphere are preserved in the sutures, which define the places where the ancient oceans disappeared. Oceanic lithosphere may also comprise obducted topographic highs, such as seamounts and oceanic islands that are built on top of it. During closure of an ocean, these structures are partly carried along with the subducting oceanic lithosphere, while some portion of them gets integrated into the subduction/accretion complex which may contain rocks of varying origins, including fragments of oceanic crust, oceanic lithospheric mantle and seamounts/oceanic islands. This, in turn, may result in highly heterogeneous lithological assemblage encompassing a wide spectrum of geochemical signatures (including N-MORB-, E-MORB- and OIB-types).

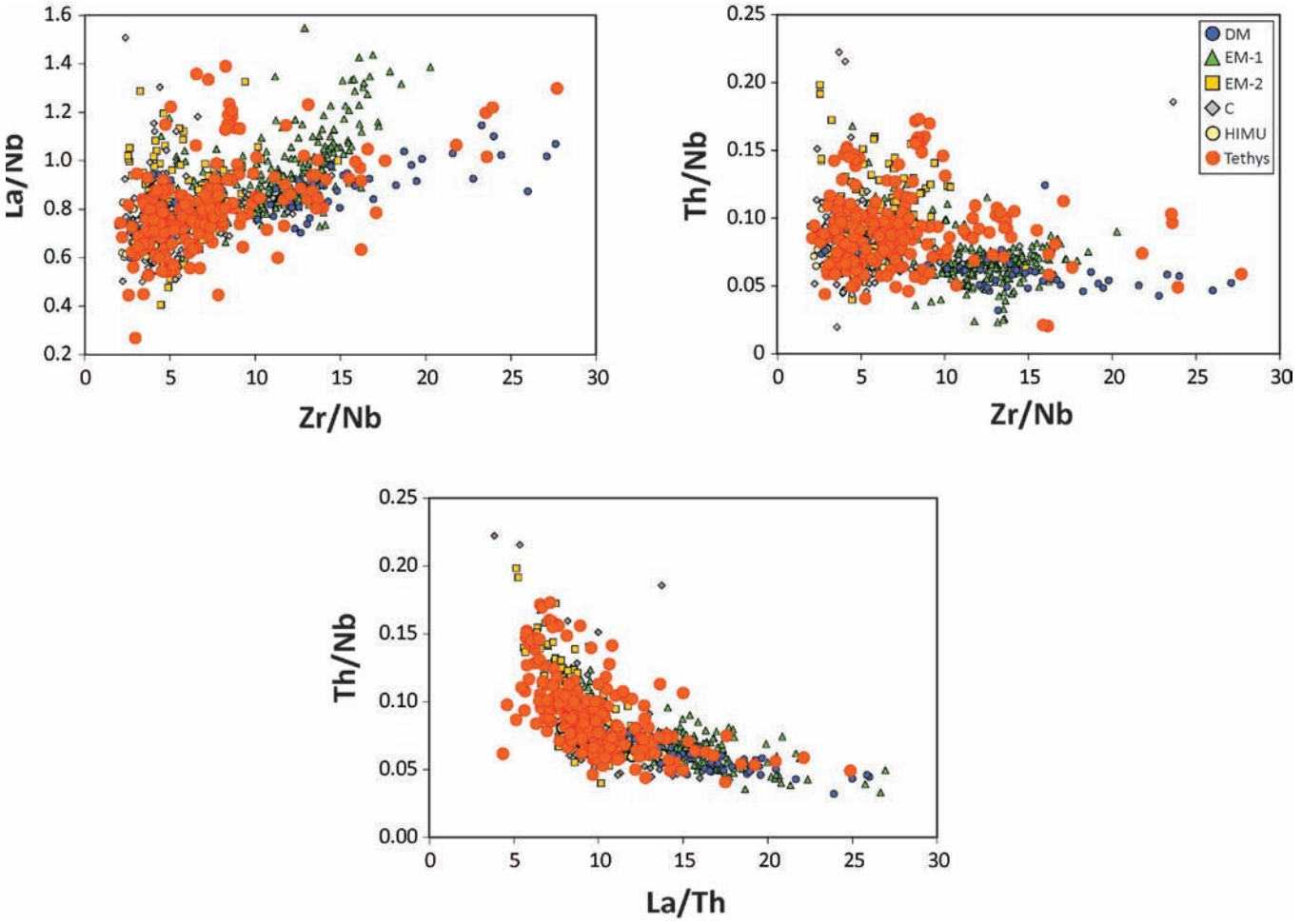

Fig. 7 - Distribution of the OIB- and E-MORB-type Tethyan samples compared with the modern OIBs. Regarding the Tethyan samples, only those with MgO > 5 were shown on the plots. No change was applied for the modern OIB samples; they are the same as shown in the previous figures. A lower filtering value was applied for the Tethyan samples in order to keep maximum number of samples. Tethyan data were compiled from Li et al. (2002), Lapierre et al. (2004), Rojay et al. (2004), Saccani and Photiades (2005), Aldanmaz et al. (2008), Maury et al. (2008), Xia et al. (2008), Bagheri and Stampfli (2008), Xiao et al. (2008), Bedard et al. (2009), Göncüoglu et al. (2010), Sayit et al. (2010), Dai et al. (2011) and unpublished data of the present author.

Remnants of Tethyan oceans are among the best examples in the world, which comprise fragments of ancient oceanic lithosphere as well as structures attached to it (e.g., Bortolotti et al., 2004; Saccani and Photiades, 2005; Sayit et al., 2010). Enriched trace element signatures (E-MORB- and OIB-type) are not uncommon, and can be found in several places around the world within the Tethyan suture zones, such as the Karakaya Complex (Palaeotethys, Turkey), Izmir-Ankara-Erzican Suture Zone (Neotethys, Turkey), Antalya Nappes (Neotethys, Turkey), Yarlung Zangbo Suture Zone (Palaeotethys, Neotethys, China), Variscan Accretionary Complex (Palaeotethys, Iran), Xiaru-Tuoding Area (Palaeotethys, China), Albanide-Hellenide Orogenic Belt (Neotethys, Greece), Hawasina Nappes and Saih Hattat Window (Neotethys, Oman) (e.g., Lapierre et al., 2004; Saccani and Photiades, 2005; Aldanmaz et al., 2008; Bagheri and Stampfli, 2008; Maury et al., 2008; Xia et al., 2008; Xiao et al., 2008; Sayit et al., 2010; Dai et al., 2011).

When the Tethyan samples (compiled from the areas mentioned above) are plotted together with modern OIBs, it is observed that Tethyan samples are unable to fully cover the modern OIB range (Fig. 7). While this can be simply a consequence of sampling bias, the Tethyan samples still reflect extensive ranges in terms of immobile trace element ratios. Such geochemical variety may imply existence of a heterogeneous mantle underlying the Tethyan basins, which is also supported by isotopic data (e.g., Mahoney et al., 1998; Xu et al., 2002; Xu and Castillo, 2004; Lapierre et al., 2004; Maury et al., 2008). Similar to what is observed from the modern OIB magmatism, the heterogeneity of the Tethyan magmatism may also have resulted from the involvement of recycled oceanic lithosphere carried by mantle plumes. Fragments of this material may also have dispersed (as streaks) throughout the Tethyan upper mantle. Mantle plumes appear to have played an active role in shaping the Tethyan magmatism, and they may have been an important factor in the opening of both Palaeotethys and Neotethys (e.g., Wilson et al., 1998; Lapierre et al., 2004; Sayit and Göncüoglu, 2009).

CONCLUSIONS

Combined trace element and isotope systematics suggest that the origin of the distinct melts reflecting diverse end-member signatures can be explained by involvement of metasomatized oceanic lithosphere (crust + mantle part) with/without sediment content. Sole involvement of eclogitic lithologies cannot account for trace element systematics of OIBs; a peridotitic component is needed in the genesis of all end-member signatures. This result would be consistent with the idea of recycling of oceanic lithosphere and its rise as a mantle plume (e.g., Hofmann and White, 1982; Lassiter and Hauri, 1998; Chauvel et al., 2008). Melting of peridotitic and eclogitic lithologies within the oceanic lithosphere and the subsequent mixing of created melts can explain the trace element and isotope systematics of OIBs. The diverse trace element signatures reflected by the Tethyan samples suggest that similar processes may have also operated in creating the heterogeneity observed in the Tethyan realm, where recycled oceanic lithosphere was the key component.

ACKNOWLEDGEMENTS

I appreciate the reviews by Paola Tartarotti and Alessandra Mantonini, which greatly improved the manuscript. I am grateful to Luca Pandolfi for his editorial efforts. I also thank Tanya Furman and Barry Hanan for the useful discussions on the earlier versions of the manuscript.

REFERENCES

Aldanmaz E., Yaliniz M.K., Güctekin A. and Göncüoglu M.C., 2008. Geochemical characteristics of mafic lavas from the Neotethyan ophiolites in western Turkey: implications for heterogeneous source contribution during variable stages of ocean crust generation. Geol. Mag., 145: 37-54.

Allègre C.J. and Turcotte D.L., 1986. Implications of a two-component marble-cake mantle. Nature, 323: 123-127.

Bagheri S. and Stampfli G.M., 2008. The Anarak, Jandaq and Posht-e-Badam metamorphic complexes in central Iran: New geological data, relationships and tectonic implications. Tectonophysics, 451: 123-155.

Bédard J.H., 1994. A procedure for calculating the equilibrium distribution of trace elements among the minerals of cumulate rocks, and the concentration of trace elements in the coexisting liquids. Chem. Geol., 118: 143-153.

Bédard E., Hebert R., Guilmette C., Lesage G., Wang C.S. and Dostal J., 2009. Petrology and geochemistry of the Saga and Sangsang ophiolitic massifs, Yarlung Zangbo Suture Zone, Southern Tibet: Evidence for an arc-back-arc origin. Lithos, 113: 48-67.

Blundy J. and Wood B., 2003. Mineral-melt partitioning of uranium, thorium and their daughters. Rev. Mineral. Geochem., 52: 59-123.

Bodinier J.L., 1988. Geochemistry and petrogenesis of the Lanzo peridotite body, western Alps. Tectonophysics, 149: 67-88.

Bortolotti V., Chiari M., Marcucci M., Marroni M., Pandolfi L., Principi G. and Saccani E., 2004. Comparison among the Albanian and Greek Ophiolites: In search of constraints for the evolution of the Mesozoic Tethys Ocean. Ofioliti, 29 (1): 19-35.

Chauvel C., Hofmann A.W. and Vidal P., 1992. HIMU-EM: The French Polynesia connection. Earth Planet. Sci. Lett., 110: 99-119.

Chauvel C., Lewin E., Carpentier M., Arndt N.T. and Marini J-C., 2008. Role of recycled oceanic basalt and sediment in generating the Hf-Nd mantle array. Nature Geosci., 1: 64-67.

Chen C-Y. and Frey F.A. 1985. Trace element and isotopic geochemistry of lavas from Haleakala Volcano, East Maui, Hawaii: Implications for the origin of Hawaiian basalts. J. Geophys. Res., 90: 8743-8768.

Christensen U.R. and Hofmann A.W., 1994. Segregation of subducted oceanic crust in the convecting mantle. J. Geophys. Res., 99: 19867-19884.

Class C., Miller D.M., Goldstein S.L. and Langmuir C.H., 2000. Distinguishing melt and fluid subduction components in Umnak Volcanics, Aleutian Arc. Geochem. Geophys. Geosyst., 1: 1999GC000010.

Collerson K.D., Williams Q., Ewart A.E. and Murphy D.T., 2010. Origin of HIMU and EM-1 domains sampled by ocean island basalts, kimberlites and carbonatites: The role of CO_2-fluxed lower mantle melting in thermochemical upwellings. Phys. Earth Planet. Inters., 181: 112-131.

Condie K.C., 2005. High field strength element ratios in Archean basalts: a window to evolving sources of mantle plumes? Lithos, 79: 491-504.

Dai J., Wang C., Hebert R., Li Y., Zhong H., Guillaume R., Bezard R. and Wei Y., 2011. Late Devonian OIB alkaline gabbro in the Yarlung Zangbo Suture Zone: Remnants of the Paleo-Tethys?. Gondwana Res., 19: 232-243.

Dasgupta R., Hirschmann, M.M. and Withers A.C., 2004. Deep global cycling of carbon constrained by the solidus of anyhdrous, carbonated eclogite under upper mantle conditions. Earth Planet. Sci. Letts., 227: 73-85.

Dixon J.E., Leist L., Langmuir C. and Schilling J-G., 2002. Recycled dehydrated lithosphere observed in plume-influenced mid-ocean-ridge basalt. Nature, 420: 385-389.

Donnelly K.E., Goldstein S.L., Langmuir C.H. and Spiegelman M., 2004. Origin of enriched ocean ridge basalts and implications for mantle dynamics. Earth Planet. Sci. Lett., 226: 347-366.

Dupre B. and Allègre C.J., 1983. Pb-Sr isotope variation in Indian Ocean basalts and mixing phenomena. Nature, 303: 142-146.

Eisele J., Sharma M., Galer S.J.G., Blichert-Toft J., Devey C.W. and Hofmann A.W., 2002. The role of sediment recycling in EM-1 inferred from Os, Pb, Hf, Nd, Sr isotope and trace element systematics of the Pitcairn hotspot. Earth Planet. Sci. Lett., 196: 197-212.

Fabriès J., Lorand J.P. and Bodinier J.L. 1998. Petrogenetic evolution of orogenic lherzolite massifs in the central and western Pyrenees. Tectonophysics 292: 145-167.

Farley K.A., Natland J.H. and Craig H., 1992. Binary mixing of enriched and undegassed (primitive?) mantle components (He, Sr, Nd, Pb) in Samoan lavas. Earth. Planet. Sci. Lett., 111: 183-199.

Frey F.A. and Rhodes J.M., 1993. Intershield geochemical differences among Hawaiian volcanoes: implications for source compositions, melting process and magma ascent paths. Philos. Trans. R. Soc. London, A, 342: 121-136.

Fukao Y., Obayashi M. and Nakakuki T., 2009. Deep Slab Project Group. Stagnant slab: A review. Ann. Rev. Earth Planet. Sci., 37: 19-46.

Fukao Y., Wildiyantoro S. and Obayashi M., 2001. Stagnant slabs in the upper and lower mantle transition region. Rev. Geophys., 39: 291-323.

Gaffney A.M., Nelson B.K. and Blichert-Toft J., 2004. Geochemical constraints on the role of oceanic lithosphere in intra-volcano heterogeneity at West Maui, Hawaii. J. Petrol., 45: 1663-1687.

Göncüoglu M.C., Sayit K. and Tekin U.K., 2010. Oceanization of the northern Neotethys: Geochemical evidence from ophiolitic mélange basalts within the İzmir-Ankara suture belt, NW Turkey: Lithos, 116: 175-187.

Green T.H., Green D.H. and Ringwood A.E., 1967. The origin of high-alumina basalts and their relationships to quartz tholeiites and alkali basalts: Earth Planet. Sci. Lett., 2: 41-51.

Haase K.M., Stoffers P. and Garbe-Schönberg C.D., 1997. The petrogenetic evolution of lavas from Easter Island and neighbouring seamounts, near-ridge hotspot volcanoes in the SE Pacific. J. Petrol., 38: 785-813.

Hanan B.B. and Graham D.W., 1996. Lead and Helium isotope evidence from oceanic basalts for a common deep source of mantle plumes. Science, 272: 991-995.

Hart S.R., 1984. A large-scale isotope anomaly in the Southern Hemisphere mantle. Nature, 309: 753-757.

Hart S.R. and Dunn T., 1993. Experimental cpx/melt partitioning of 24 trace elements. Contrib. Mineral. Petrol., 113: 1-8.

Hart S.R., Hauri E.H., Oschmann L.A. and Whitehead J.A., 1992. Mantle plumes and entrainment: isotopic evidence. Science, 256: 517-520.

Hawkesworth C.J., Gallagher K., Hergt J.M. and Mcdermott F., 1993. Trace element fractionation processes in the generation of island arc basalts. Philos. Trans. R. Soc. London, A, 342: 179-191.

Hemond C., Devey C.W. and Chauvel C., 1994. Source compositions and melting processes in the Society and Austral plumes (South Pacific Ocean): Element and isotope (Sr, Nd, Pb, Th) geochemistry. Chem. Geol., 115: 7-45.

Hirose K., Takafuji N., Nagayoshi S. and Ohishi Y., 2005. Phase transition and density of subducted MORB crust in the lower mantle. Earth Planet. Sci. Lett., 237: 239-251.

Hirschmann M.M. and Stolper E.M., 1996. A possible role for garnet pyroxenite in the origin of the "garnet signature" in MORB. Contrib. Mineral. Petrol., 124: 185-208.

Hirschmann M.M., Kogiso T., Baker M.B. and Stolper E.M., 2003. Alkalic magmas generated by partial melting of garnet pyroxenite. Geology, 31: 481-484.

Hofmann A.W. and Hart S.R., 1978. An assessment of local and regional isotopic equilibrium in the mantle. Earth Planet. Sci. Lett., 38: 44-62.

Hofmann A.W. and Jochum K.P., 1996. Source characteristics derived from very incompatible trace elements in Mauna Loa and Mauna Kea basalts, Hawaii Scientific Drilling Project. J. Geophys. Res., 101: 11831-11839.

Hofmann A.W. and White W.M., 1982. Mantle plumes from ancient oceanic crust. Earth Planet. Sci. Lett., 57: 421-436.

Ito G. and Mahoney J.J. 2005. Flow and melting of a heterogeneous mantle: 1. Method and importance to the geochemistry of ocean island and mid-ocean ridge basalts. Earth Planet. Sci. Lett., 230: 29-46.

Jackson M.G. and Dasgupta R. 2008. Compositions of HIMU, EM1, and EM2 from global trends between radiogenic isotopes and major elements in ocean island basalts. Earth Planet. Sci. Lett., 276: 175-186.

Jackson M.G., Hart S.R., Koppers A.A.P., Staudigel H., Konter J., Blusztajn J., Kurz M. and Russell J.A., 2007. The return of subducted continental crust in Samoan lavas. Nature, 448: 684-687.

Johnson K.T.M., 1998. Experimental determination of partition coefficients for rare earth and high-field-strength elements between clinopyroxene, garnet, and basaltic melt at high pressures. Contrib. Mineral. Petrol., 133: 60-68.

Johnson M.C. and Plank T., 1999. Dehydration and melting experiments constrain the fate of subducted sediments. Geochem. Geophys. Geosyst., 1, doi:10.1029/1999GC000014.

Kelemen P.B., Shimizu N. and Dunn T., 1993. Relative depletion of niobium in some arc magmas and the continental crust: partitioning of K, Nb, La and Ce during melt/rock reaction in the upper mantle. Earth Planet. Sci. Lett., 120: 111-134.

Kellogg L.H., Hager B.H. and van der Hilst R.D., 1999. Compositional stratification in the deep mantle: Science, 283: 1881-1884.

Klemme S., Blundy J.D. and Wood B.J., 2002. Experimental constraints on major and trace element partitioning during partial melting of eclogite. Geochim. Cosmochim. Acta, 66: 3109-3123.

Klemme S., Prowatke S., Hematner K. and Gunther D., 2005. Partitioning of trace elements between rutile and silicate melts: Implications for subduction zones. Geochim. Cosmochim. Acta, 69: 2361-2371.

Kogiso T. and Hirschmann M.M., 2006. Partial melting experiments of bimineralic eclogite and the role of recycled mafic oceanic crust in the genesis of ocean island basalts. Earth Planet. Sci. Lett., 249: 188-199.

Kogiso T., Hirschmann M.M. and Frost D.J., 2003. High-pressure partial melting of garnet pyroxenite:possible mafic lithologies in the source of ocean island basalts. Earth Planet. Sci. Lett., 216: 603-617.

Kostopoulos D.K. and Murton B.J., 1992. Origin and distribution of components in boninite genesis: significance of the OIB component. In: L.M. Parson, B.J. Murton and M.J. Norry (Eds.), Ophiolites and theirmodern oceanic analogues. Geol. Soc. London Spec. Publ., 60: 133-154.

Lapierre H., Samper A., Bosch D., Maury R.C., Béchennec F., Cotten J., Demant A., Brunet P., Keller F. and Marcoux J., 2004. The Tethyan plume: geochemical diversity of Middle Permian basalts from the Oman rifted margin. Lithos, 74: 167-198.

Lassiter J.C. and Hauri E.H., 1998. Osmium-isotope variations in Hawaiian lavas: evidence for recycled oceanic lithosphere in the Hawaiian plume. Earth Planet. Sci. Lett., 164: 483-496.

Li X-H., Zhou H., Chung S-L., Ding S., Liu Y., Lee C-Y, Ge W., Zhang Y. and Zhang R., 2002. Geochemical and Sm-Nd isotopic characteristics of metabasites from central Hainan Island, South China and their tectonic significance. Isl. Arc, 11: 193-205.

Ludden J., Gelinas L. and Trudel P., 1982. Archean metavolcanics from the Rouyn-Noranda district, Abitibi Greenstone Belt, Quebec. 2. Mobility of trace elements and petrogenetic constraints. Can. J. Earth Sci., 19: 2276-2287.

Mahoney J.J., Frei R., Tejada M.L.G., Mo X.X., Leat P.T. and Nagler T.F., 1998. Tracing the Indian Ocean mantle domain through time: Isotopic results from old West Indian, East Tethyan, and South Pacific Seafloor. J. Petrol., 39: 1285-1306.

Maruyama S., Santosh M. and Zhao D., 2007. Superplume, supercontinent, and post-perovskite: Mantle dynamics and anti-plate tectonics on the core-mantle boundary. Gondwana Res., 11: 7-37.

Maury R.C., Lapierre H., Bosch D., Marcoux J., Krystyn L., Cotten J., Bussy F., Brunet P. and Senebier F., 2008. The alkaline intraplate volcanism of the Antalya nappes (Turkey): a Late Triassic remnant of the Neotethys. Bull. Soc. Géol. France, 179: 397-410.

McKenzie D. and O'Nions R.K., 1991. Partial melt distributions from inversion of rare earth element concentrations. J. Petrol., 32: 1021-1091.

Montanini A, Tribuzio R. and Thirlwall M., 2012. Garnet clinopyroxenite layers from the mantle sequences of the Northern Apennine ophiolites (Italy): evidence for recycling of crustal material. Earth Planet. Sci. Lett., 351-352: 171-181.

Morgan J.P., 1999. Isotope topology of individual hotspot basalt arrays: Mixing curves or melt extraction trajectories? Geochem. Geophys. Geosyst., 1, paper n.: 1999GC000004.

Morgan J.P. and Morgan W.J., 1999. Two-stage melting and the geochemical evolution of the mantle: a recipe for mantle plum-pudding. Earth Planet. Sci. Lett., 170: 215-239.

Niu Y. and O'Hara M.J., 2003. Origin of ocean island basalts: A new perspective from petrology, geochemistry, and mineral physics considerations. J. Geophys. Res., 108, doi: 10.1029/2002JB002048.

Niu Y., Collerson K.D., Batiza R., Wendt J.I. and Regelous M., 1999. Origin of enriched-type mid-ocean rigde basalt at ridges far from mantle plumes: The East Pacific Rise at 11°20'N. J. Geophys. Res., 104: 7067-7087.

Pearce J.A., 2008. Geochemical fingerprinting of oceanic basalts with applications to ophiolite classification and the search for Archean oceanic crust. Lithos, 100: 14-48.

Pearce J.A. and Cann J.R., 1973. Tectonic setting of basic volcanic rocks determined using trace element analysis. Earth Planet. Sci. Lett., 19: 290-300.

Pearce J.A. and Peate D.W., 1995. Tectonic implications of the composition of volcanic arc magmas: Ann. Rev. Earth Planet. Sci., 23: 251-285.

Pearson D.G., Davies G.R. and Nixon P.H., 1993. Geochemical constraints on the petrogenesis of diamond facies pyroxenites from the Beni Bousera peridotite massif, north Morocco. J. Petrol., 34: 125-172.

Pertermann M. and Hirschmann M.M., 2003. Partial melting experiments on a MORB-like pyroxenite between 2 and 3 Gpa: Constraints on the presence of pyroxenite in basalt source regions from solidus location and melting rate. J. Geophys. Res., 108 (B2); doi:10.1029/2000JB000118.

Pfänder J.A., Münker C., Stracke A. and Mezger K., 2007. Nb/Ta and Zr/Hf in ocean island basalts - Implications for crust-mantle differentiation and the fate of Niobium. Earth Planet. Sci. Lett., 254: 158-172.

Pilet S., Hernandez J., Slyvester P. and Poujol M., 2005. The metasomatic alternative for ocean island basalt chemical heterogeneity. Earth Planet. Sci. Lett., 236: 148-166.

Plank T. and Langmuir C.H., 1998. The chemical composition of subducting sediment and its consequences for the crust and mantle. Chem. Geol., 145: 325-394.

Porter K.A. and White W.M., 2009. Deep mantle subduction flux. Geochem. Geophys. Geosyst., 10, doi:10.1029/2009GC002656.

Prendergast E. and Offler R., 2012. Underplated seamount in the Narooma accretionary complex, NSW, Australia. Lithos, 154: 224-234.

Rojay B., Altiner D., Ozkan Altiner S., Onen A.P., James S. and Thirlwall M.F., 2004. Geodynamic significance of the Cretaceous pillow basalts from North Anatolian Ophiolitic Mélange Belt (Central Anatolia, Turkey): geochemical and paleontological constraints. Geodin. Acta, 17 (5): 349-361.

Saccani E. and Photiades A., 2005. Petrogenesis and tectonomagmatic significance of volcanic and subvolcanic rocks in the Albanide-Hellenide ophiolitic mélanges. Isl. Arc, 14: 494-516.

Salters V.J.M. and Longhi J., 1999. Trace element partitioning during the initial stages of melting beneath mid-ocean ridges. Earth Planet. Sci. Lett., 166: 15-30.

Salters V.J.M., Longhi J.E. and Bizimis M., 2002. Near mantle solidus trace element partitioning at pressures up to 3.4 GPa. Geochem. Geophys. Geosyst., 3, doi:10.1029/2009GC002656.

Sayit K. and Göncüoglu M.C. 2009. Geochemistry of mafic rocks of the Karakaya Complex, Turkey: Evidence for plume-involvement in the extensional oceanic regime during Middle-Late Triassic. Int. J. Earth Sci., 98: 367-385.

Sayit K., Göncüoglu M.C. and Furman T., 2010. Petrological reconstruction of Triassic seamounts/oceanic islands within the Palaeotethys: Geochemical implications from the Karakaya subduction/accretion Complex, Northern Turkey. Lithos, 119: 501-511.

Shaw D.M., 2006. Trace elements in magmas: A theoretical treatment, Cambridge Univ., Cambridge.

Sobolev A.V., Hofmann A.W., Kuzmin D.V. et al., 2007. The amount of recycled crust in the sources of mantle-derived melts. Science, 316: 412-417.

Sobolev A.V., Hofmann A.W. and Nikogosian I.K., 2000. Recycled oceanic crust observed in 'ghost plagioclase' within the source of Mauna Loa lavas. Nature, 404: 986-990.

Sobolev A.V., Hofmann A.W., Sobolev S.V. and Nikogosian I.K., 2005. An olivine-free mantle source of Hawaiian shield basalts. Nature, 434: 590-597.

Staudigel H., Plank T., White B. and Schmincke H-U., 1996. Geochemical fluxes during seafloor alteration of the basaltic upper oceanic crust: DSDP sites 417 and 418. Geophys. Monogr. Ser., 96: 19-38.

Stracke B. and Bourdon B., 2009. The importance of melt extraction for tracing mantle heterogeneity. Geochim. Cosmochim. Acta, 73: 218-238.

Stracke A., Bizimis M. and Salters V.J.M., 2003. Recycling oceanic crust: Quantitative constraints. Geochem. Geophys. Geosyst., 4, doi: 10.1029/2001GC000148.

Stracke A., Hofmann A.W. and Hart S.R., 2005. FOZO, HIMU, and the rest of the mantle zoo. Geochem. Geophys. Geosyst., 6, doi: 10.1029/2004GC000824.

Suen C.J. and Frey F.A., 1987. Origins of the mafic and ultramafic rocks in the Ronda peridotite. Earth Planet. Sci. Lett., 85: 183-202.

Sun S-S. and McDonough W.F., 1989. Chemical and isotopic systematics of oceanic basalts: implications for mantle composition and processes. In: A.D. Saunders and MJ Norry (Eds.), Magmatism in the ocean basins. Geol. Soc. London Spec. Publ., 42: 313-345.

Tatsumi Y., 1989. Migration of fluid phases and genesis of basalt in subduction zones. J. Geophys. Res., 94: 4697-4707.

van Westrenen W., Blundy J.D. and Wood B.J., 1999. Crystal-chemical controls on trace element partitioning between garnet and anhydrous silicate melt. Am. Mineral., 84: 838-847.

Volkova N.I. and Budanov V.I., 1999. Geochemical discrimination of metabasalt rocks of the Fan-Karategin transitional blueschist/greenschist belt, South Tianshan, Tajikistan: seamount volcanism and accretionary tectonics. Lithos, 47: 201-216.

Weaver B.L., 1991. The origin of ocean island basalt end-member compositions: trace element and isotopic constraints. Earth Planet. Sci. Lett., 104: 381-397.

White W.M., 1985. Sources of oceanic basalts: Radiogenic isotopic evidence. Geology, 13: 115-118.

White W.M., 2010. Oceanic island basalts and mantle plumes: The geochemical perspective. Ann. Rev. Earth Planet. Sci., 38: 133-160.

White W.M. and Hofmann A.W., 1982. Sr and Nd isotope geochemistry of oceanic basalts and mantle evolution. Nature, 296: 821-825.

Wilson M. and Guiraud R., 1998. Late Permian to recent magmatic activiy on the African-Arabian margin of Tethys. In: D.S. Macgregor, R.T.J. Moody and D.D. Clark-Lowes (Eds.), Petroleum geology of North Africa. Geol. Soc. London Spec. Publ., 132: 231-263.

Woodhead J.D., 1996. Extreme HIMU in an oceanic setting: the geochemistry of Mangaia Island (Polynesia), and temporal evolution of the Cook-Austral hotspot. J. Volcan. Geotherm. Res., 72: 1-19.

Workman R.K. and Hart S.R., 2005. Major and trace element composition of the depleted MORB mantle (DMM). Earth Planet. Sci. Lett., 231: 53-72.

Workman R.K., Hart S.R., Jackson M., Regelous M., Farley K.A., Blusztajn J., Kurz M., and Staudigel H., 2004. Recycled metasomatized lithosphere as the origin of the enriched mantle II (EM2) end-member: Evidence from the Samoan volcanic chain. Geochem. Geophys. Geosyst., 5, doi: 10.1029/2003GC000623.

Xia B., Chen G-W., Wang R. and Wang Q., 2008. Seamount volcanism associated with the Xigaze ophiolite, Southern Tibet. J. Asian Earth Sci., 32: 396-405.

Xiao L., He Q., Pirajno F., Ni P., Du J. and Wei Q., 2008. Possible correlation between a mantle plume and the evolution of Palaeo-Tethys Jinshajiang Ocean: Evidence from a volcanic rifted margin in the Xiaru-Tuoding area, Yunnan, SW China. Lithos, 100: 112-126.

Xu J-f. and Castillo P.R., 2004. Geochemical and Nd-Pb isotopic characteristics of the Tethyan astenosphere: implications for the origin of the Indian Ocean mantle domain. Tectonophyics, 393: 9-27.

Xu J-f., Castillo P.R., Li X-h., Yu X-y., Zhang B-r. and Han Y-w., 2002. MORB-type rocks from the Paleo-Tethyan Mian-Lueyang northern ophiolite in the Qinling Mountains, central China: implications for the source of the low $^{206}Pb/^{204}Pb$ and high $^{143}Nd/^{144}Nd$ mantle component in the Indian Ocean. Earth Planet. Sci. Lett., 198: 323-337.

Zindler A. and Hart S., 1986. Chemical geodynamics. Ann. Rev. Earth. Planet. Sci., 4: 493-571.

Zindler A., Staudigel H. and Batiza R., 1984. Isotope and trace element geochemistry of young Pacific seamounts: Implications for the scale of upper mantle heterogeneity. Earth Planet. Sci. Lett., 70: 175-195.

Received, November 22, 2013
Accepted, May 15, 2013